C. R. Physique 12 (2011) 387–416

Contents lists available at ScienceDirect

Comptes Rendus Physique

www.sciencedirect.com

Article for the 50th anniversary of the invention of the LASER

Science and technology challenges in XXIst century optical communications

Challenges scientifiques et technologiques des télécommunications optiques du XXIème siècle

E. Desurvire [a,*], C. Kazmierski [b], F. Lelarge [b], X. Marcadet [b], André Scavennec [b], F.A. Kish [c], D.F. Welch [c], R. Nagarajan [c], C.H. Joyner [c], R.P. Schneider Jr. [c], S.W. Corzine [c], M. Kato [c], P.W. Evans [c], M. Ziari [c], A.G. Dentai [c], J.L. Pleumeekers [c], R. Muthiah [c], S. Bigo [d], M. Nakazawa [e], D.J. Richardson [f], F. Poletti [f], M.N. Petrovich [f], S.U. Alam [f], W.H. Loh [f], D.N. Payne [f]

[a] *Thales Research & Technology, Physics Research Group, Campus de Polytechnique, 1, avenue Augustin Fresnel, 91767 Palaiseau cedex, France*
[b] *Alcatel-Thales III-V Lab, joint laboratory of Alcatel-Lucent Bell Labs France and Thales Research & Technology, route de Nozay, 91460 Marcoussis, France*
[c] *Infinera Corporation, 1322 Bordeaux Drive, Sunnyvale, CA 94089, USA*
[d] *Alcatel-Lucent, Bell Labs, Centre de Villarceaux, 91620 Nozay, France*
[e] *Tohoku University, Research Institute of Electrical Communication, Sendai, Japan*
[f] *Optoelectronics Research Centre, University of Southampton, Southampton SO17 1BJ, UK*

ARTICLE INFO

Article history:
Received 8 April 2011
Accepted after revision 8 April 2011

Keywords:
Erbium-doped fibre amplifier
Modulation format
Optical telecommunications
Photonics
Shannon limit
Wavelength-division multiplexing

Mots-clés :
Amplificateur à fibre dopée à l'erbium
Format de modulation
Photonique
Limite de Shannon
Multiplexage en longueur d'onde
Télécommunications optiques

ABSTRACT

The state of the art of XXIst century optical communication systems is reviewed through the associated technologies of laser sources, photo-receivers, integrated photonic circuits, optical fibres, and coherent modulation formats. Emphasis is put on current science and technology challenges to approach ultimate physical limits and to develop innovative solutions allowing performance enhancement at minimal cost increase.

RÉSUMÉ

Cette présentation passe en revue l'état de l'art des systèmes de télécommunications optiques du XXIème siècle à travers les technologies des sources lasers, des photorécepteurs, des circuits photoniques intégrés, des fibres optiques, et des formats de modulation cohérents. L'accent y est placé sur les challenges scientifiques et technologiques posés par l'approche des limites physiques ultimes et par le développement de solutions innovantes permettant l'augmentation des performances au moindre coût.

* Corresponding author.
E-mail addresses: emmanuel.desurvire@thalesgroup.com (E. Desurvire), christophe.kazmierski@3-5lab.fr (C. Kazmierski), fkish@infinera.com (F.A. Kish), sebastien.bigo@alcatel-lucent.com (S. Bigo), nakazawa@riec.tohoku.ac.jp (M. Nakazawa), djr@orc.soton.ac.uk (D.J. Richardson).

1631-0705/$ – see front matter
doi:10.1016/j.crhy.2011.04.009

Nomenclature

A/D	Analog-to-digital
ADC	Analog-to-digital converter
APD	Avalanche photo-diode
ASE	Amplified spontaneous emission
ASIC	Application-specific integrated circuit
AWG	Arbitrary waveform generator
AWG	Arrayed waveguide grating
BER	Bit error rate
BT	British Telecom
CAGR	Compound annual growth rate
CD	Chromatic dispersion
CMA	Constant-modulus algorithm
CVD	Chemical vapour deposition
CW	Continuous laser
CWA	Chemical weapon agent
DFB	Distributed Feed-Back
DGE	Dynamic gain equaliser
DGD	Differential group delay
DIRCM	Directed counter-measure
DM	Dispersion management
DML	Directly modulated laser
DPSK	Differential phase-shift keying
DVD	Digital video disk
E-PSCF	Enhanced pure silica-core fibre
EA	Electro-absorption
EDFA	Erbium-doped fibre amplifier
EML	Electro-absorption modulated laser
FEC	Forward Error correction
FIR	Finite impulse response
FIT	Failure in time
FM	Frequency modulation
FP	Fabry–Pérot
FSK	Frequency shift keying
HNL-DFF	Highly-nonlinear dispersion-flattened fibre
I-Q	Cosine-sine (components)
IC	Integrated circuit
ICT	Information and communication technologies
IDF	Inverse dispersion fibre
IF	Intermediate frequency
IR	Infrared
ISD	Information spectral density
ITU	International Telecommunication Union
LASER	Light amplification by stimulated emission of radiation
LD	Laser diode
LO	Local oscillator
MLFL	Mode-locked fibre laser
MLL	Mode-locked laser
MOCVD	Metal-organic chemical vapour deposition
NRZ	Non-return to zero
O/E	Optoelectronic
OCM	Optical counter-measure
OEIC	Optoelectronic integrated circuit
OFDM	Optical frequency-division multiplexing
OFT	Optical Fourier transform
OFTC	Optical Fourier transform circuit
OML	Optical Moore's Law
OOK	On-Off keying
OPLL	Optical phase-locked loop
OSNR	Optical signal-to-noise ratio
OTDM	Optical time division multiplexing
P-DPSK	Partial differential phase-shift keying
PBGF	Photonic-bandgap fibre
PC	Polarisation controller
PIA	Phase-insensitive amplifier/amplification
PIC	Photonic integrated circuit
PDM	Polarisation division multiplexing
PLL	Phase-locked loop
PM	Polarisation multiplexing
PMD	Polarisation mode dispersion
PMF	Polarisation-maintaining fibre
POL-MUX	Polarisation multiplexing
PPG	Pulse-pattern generator
PRBS	Pseudo-random bit sequence
PSA	Phase-sensitive amplifier/amplification
PSK	Phase shift keying
PSP	Principal state of polarisation
QAM	Quadrature-amplitude modulation
QCL	Quantum cascade laser
QD	Quantum dot/dash
QPSK	Quadrature-phase-shift-keying
QW	Quantum well
RE	Rare earth
RF	Radio frequency
RT	Room temperature
RZ	Return-to-zero
S-QW	Single quantum well
SAGM	Separate absorption grading and multiplication
SMF	Single-mode fibre
SMSR	Side-mode suppression ratio
SMZ	Symmetric Mach–Zehnder
SNR	Signal-to-noise ratio
SSPM	Self-phase modulation
SMF	Standard single-mode fibre
TEC	Thermal electric cooler
TIC	Toxic industrial chemical
VOA	Variable optical attenuator
WDM	Wavelength-Division Multiplexing
WPE	Wall plug efficiency

1. Introduction

1.1. Highlights on optical telecommunications history

The realisation by Corning Glass, in 1970, of the first low-loss fibres which had been predicted in 1966 by K.C. Kao and G. Hockham [1], and the parallel invention of semiconductor laser diodes and photo-detectors [2] may be seen as the two parents of a newborn field, *optical telecommunications*. Compared to previous coaxial cable systems and free-space radio links, whether terrestrial or satellite, optical fibres offered an overwhelming, virtually "infinite" bandwith reservoir. Such a "bandwidth" concept means the capability to code signals and propagate them at virtually any data rate. This is because optical carriers oscillate at 200,000 GHz frequencies, to compare with MHz–GHz radio communications. Furthermore, the ultimate transparency of the fibre's ultra-pure glass made it possible to transmit such signals over distances as long as 100–150 km, with enough light photons at the fibre end to faithfully recover, regenerate or re-amplify the data.

To K.C. Kao and C.A. Hockham, such a level of achievement has been both a matter of *vision* and *challenge*. The *vision* was that fibre waveguides could be used to transmit laser-light signals. The key innovation was to surround the fibre core by a cladding of slightly lower refractive index, so as to trap the light rays by total internal reflection in the core. Through appropriate waveguide design, light is further confined into a unique electro-magnetic propagation mode, hence the name: "single-mode" fibre, or SMF. The *challenge* was then to find the proper material with which to make the fibre. Glass, such as that based on silica (of which sand is essentially composed), was the most transparent material known at the time. In the early 1960s, the best silica glass could transmit light at 0.8 μm wavelength with 20% loss, or one decibel, per meter. Such a loss figure would make a 30 m-long fibre absorb 99.9% of the signal, meaning only 1/1000th would be transmitted, which is wholly impractical from any engineering viewpoint! But in their 1966 reference, K.C. Kao and C.A. Hockham predicted that the elimination of various glass impurities could lead to much more transparent materials, with an attenuation limit near 20 dB/km, namely yielding 1/100th transmission over one kilometre of fibre. The quest for the "Holy Grail" was then engaged. As we know, the historical 20 dB/km milestone was reached only four years later (1970); but the quest for an ultimately-pure glass was not over yet. The following decade witnessed an even more spectacular domestication of fibre attenuation, as illustrated in Fig. 1. The lowest attenuation-coefficients loci in the light-transmission spectrum, would define as many successive "transmission windows" for optical telecommunications, namely: 0.8 μm, 1.1 μm, 1.3 μm and finally, 1.55 μm. Nowadays, optical fibres transmit 1.55 μm signals at a 1/10th to 1/100th levels of attenuation, but this time over 50 to 100 kilometre spans! In parallel to these phenomenal developments, compact and efficient semiconductor laser chips at 1.3 μm then 1.55 μm wavelength have been designed and qualified for efficiency, reliability, and yield, thus completing, with high-speed digital electronics, the basic optical telecommunications technology.

Since those heroic times, progress in the field has been running at a breathtaking pace, creating another "Moore's Law", as illustrated in Fig. 2. The figure shows optical-transmission performance achieved through successive technology stages (the "S-curves") in terms of Capacity $\times$ Distance (bit km/s). This means the combined error-free transmission capacity (bit/s), times the distance (km). As a reference, a 1 Gbit/s system crossing the Pacific ocean (say 10,000 km) represents a C $\times$ D of 10,000 Gbit km/s, or *10 Terabit km/s* (Tera = 1000 Giga). The figure highlights five generations in optical telecommunications history. Overlooking the first two (based upon 0.8 μm, multi-mode fibre, and the 1.3 μm SMF), we reach out to the 1.5 μm transmission window, along with its improved dispersion-compensating fibre (DSF) design. By the mid-1980s, the corresponding C $\times$ D reaches its own GIGA limit, just as the coherent-system approach, for receiver sensitivity improvement. For that matter, coherent systems were seen not to make any difference with standard direct-detection systems, much unlike twenty years after, as we shall see.

To progress any further, the stumbling stone remained *fibre loss*. Since the fibre transmission spans were, by the laws of physics, ultimately limited to 100–150 km, signals had to be electronically regenerated. This means converting the received light signals back into electrical signals, amplifying them electrically, and then reconverting them back to light by means of a complex optoelectronic device. For years on, this inescapable engineering fact represented a severe bottleneck to deploying optical networks and to fully exploiting the otherwise enormous fibre transmission capability.

Such an obstacle was overcome by the *optical fibre amplifier*. The principle consists of lightly doping the core of a short segment of fibre with an atomic element such as the rare-earth erbium. The erbium dopant has the capability to store energy and to release it as the optical signals pass through the fibre core, in accordance with Einstein's principle of stimulated emission, upon which the LASER is based. The energy release from the erbium atoms boost or re-amplify the signals, hence the name of the device, the Erbium-doped fibre amplifier, or EDFA. In order to excite the erbium atoms, one needs an auxiliary laser source, referred to as the pump. The early EDFAs were investigated around 1987–1988 by teams at the University of Southampton and Bell Laboratories [3–5]. The great challenge faced by these teams and others, was to develop a practical, efficient, and miniature pump source. Luckily, the same InGaAsP technology used in semiconductor laser diodes (LD) for optical telecommunications sources could be used for EDFA pumping once it had been redesigned to maximise power efficiency,[1] as demonstrated in 1989 by Nippon Telegraph & Telecommunications [3–5]. It is noteworthy that *the two*

[1] From an engineering perspective, the EDFA is highly power-efficient. First, the 1.55 μm laser transition is 100% radiative, i.e. without parasitic thermal-phonon relaxation. Second, the pumping efficiency, which scales as the pump-to signal photon-energy ratio (or the inverse wavelength ratio) is 95.5% and 63.2% for 1.48 μm and 980-nm pump wavelengths, respectively. Third, the semiconductor pump wall-plug efficiency (optical-to-electrical power ratio) is the

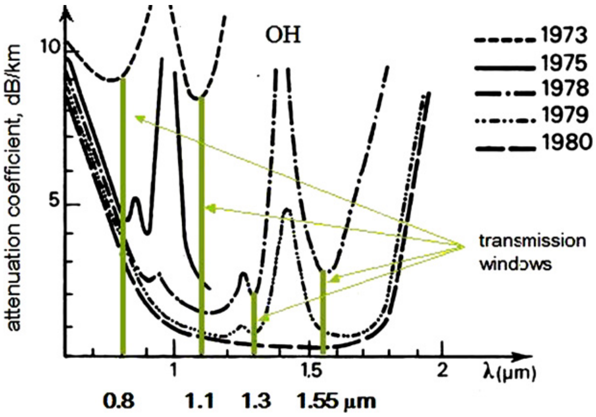

Fig. 1. Evolution though history of fibre attenuation vs. wavelength, showing four generations of *transmission windows* for fibre-optic communications, as labelled by the lowest-loss wavelength: 0.8 μm, 1.1 μm, 1.3 μm and finally 1.55 μm wavelengths (after full elimination of the “OH peak” near 1.4 μm).

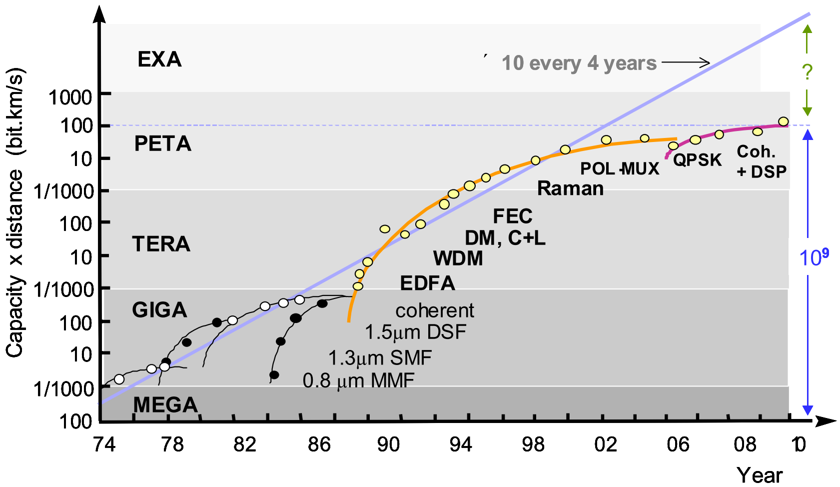

Fig. 2. Evolution through history of optical transmission-system performance, as expressed in capacity × distance (bit km/s), and according to successive technology generations. From left to right, the “S-curves” correspond to the following generations: 0.8 μm multi-mode fibre (open circles), 1.3 μm single-mode fibre (dark circles), 1.5 μm dispersion-shifted fibre (open circles), first coherent systems (dark circles), and EDFA-based systems (yellow circles/curve), with coherent multi-level formats (yellow circles/purple curve). From the time of early optical fibres (1970) to now, the capacity × distance performance has been multiplied a billion-fold. The straight blue line, showing a heuristic tenfold performance increase every four years up to year 2000, corresponds to the optical Moore’s Law. (For interpretation of the references to colour in this figure, the reader is referred to the web version of this article.)

founding technologies of optical communications, namely the laser and the fibre, could be conjoined into the EDFA, a laser-pumped, doped-fibre amplifier.

The phenomenal EDFA impact in system performance is illustrated Fig. 2. To date, telecom history has entered its TERA and the PETA (1 PETA = 1000 TERA) performance eras. The relatively sudden and unexpected availability of practical, compact and efficient, LD-pumped EDFAs made it possible to periodically regenerate signals along optical fibre links, without any optoelectronic (O/E) regeneration obstacle through the line. A single fibre could from then on seamlessly transmit optical signals over any distance from 500–1000 km up to 12,000 km, which explains the observed exponential progress.

But the EDFA came out with another striking property. When deeply saturated with high input signal loads, electronic amplifiers cause signal distortion and nonlinear mixing. In contrast, the EDFA behaves as a truly *linear* device, at least at signal bit rates of relevance. This is explained by the relatively slow dynamics of the amplifying medium (i.e. in the millisecond scale). The early investigators rapidly identified the potential of the EDFA to re-amplify several signals *at different wavelengths simultaneously* and *without any mutual interference*. Transmitting multiple signals in a single fibre in order to

---

highest possible for any lasers (typically well above 50%). Such advantageous properties are very important in the electrical power budget of EDFA-based optical communication systems, particularly in long-haul terrestrial (500–1000 km) or ultra-long-haul undersea (5000–12,000 km) applications. In the last case, terminal equipment in the class of 1 kV/1 A are capable to feed the entire system from the two continent ends. Depending upon the cable-system haul, EDFA regenerators are required every 50–70 km, the shortest spans applying to the longest. In terrestrial applications, the regenerative spans are twice, i.e. 100–150 km. In specific undersea applications called “repeaterless systems”, the EDFAs are only placed at emission (booster) and reception (pre-amplifier) ends; in such a case, optical signals may propagate without in-line regeneration over fibre distances as long as 500 km.

enhance the system's throughput capacity is referred to as *wavelength-division multiplexing*, or WDM. While the WDM approach was impractical with previous O/E regeneration, overnight it became straightforward with the introduction of the EDFA. Indeed, the erbium atoms doped into the fibre core can amplify signals at practically any data rate, as limited by the terminal's electronics. Together with the lack of inter-channel interference referred to above, thousands of billions of bits from 100–200 WDM channels could be regenerated at once in the EDFA, with perfect integrity.

In order to achieve today's system performance, however, the sole combination EDFA + WDM was hardly enough. Indeed, carrying such a huge amount of data over long ($\leqslant 1000$ km) or ultra-long fibre distances ($\leqslant 10{,}000$ km) is not at all this straightforward. This is because optical fibres exhibit a fair amount of *nonlinearity*, i.e. the refractive index becoming signal-power-dependent above a certain threshold. Fibre nonlinearity causes signal distortion, amplitude and phase noise, and disastrous WDM channel interference. On the wake of the EDFA/WDM revolution, the history of optical communications essentially turns out being the matter of "domesticating" fibre nonlinearity, together with that of fibre dispersion (through novel fibre designs), in such a way to enable transport of more and more error-free data over longer distances. Back again to Fig. 2, where the last S-curve reveals key improvements such as *dispersion management* (DM), Er-*amplifier "conventional" and "long" bands exploitation* (C + L), forward *error correction* (FEC), *Raman-amplification bandwidth upgrade* (Raman), and *polarisation multiplexing* (POL-MUX).

With all of the above incremental improvements, it has been possible to "pack" more and more data in the available fibre bandwidth, namely the EDFA or EDFA/Raman-enhanced bandwidths. After the previous O/E bottleneck, "bandwidth" became limited once again, this time by the actual number of bits that could be packed into a given slide of spectrum, be it 100 GHz or 10 THz. What follows then is the stunning return to age-old *coherent modulation/reception techniques*. These allow signal formats capable of carrying several bit-per-second-per-Hertz, such that *quadrature-phase-shift-keying* (QPSK), a variant of the more general *quadrature-amplitude modulation* (QAM). For instance, 8-QAM packs three bits into a single Hertz.

As seen at the right of Fig. 2, the suite and combination of all the above-described techniques, from EDFA/WDM to coherent, has led to the current PETA era, representing a *billion-fold improvement in transmission capability* since the inception of optical communications. It is also seen from the figure that the current S-curve dramatically departs from a heuristic "Optical Moore's Law" (OML), representing a tenfold increase every four years, which was verified until about year 2000. Since then, the gap between the OML and actual performance is a thousand-fold. According to all expectations, another S-curve should be taking over in this PETA era, with the introduction of some disruptive concepts. The key question is what these could be about, and when such a disruption may take place, [6]. Another issue, of a most fundamental nature, is that raised by Shannon's information theory: how much error-free information may be transmitted through the "*noisy optical channel*", anyway? The answer is provided by the most elegant *Shannon–Hartley theorem* [7], but the ultimate modulation formats and code systems remain yet to be discovered.

But is there any future need for more bandwidth anyway? From all operators, service providers and analysts, the answer is a solid and definitive YES! Optical fibres are now deployed worldwide across the land and along the seabed, forming a network of over *one billion kilometres* in length. Initially, the application was long-distance digital telephone and transaction data. By year 2000, the traffic demand was overtaken by the forceful emergence of a revolutionary new service, the Internet. To date, the worldwide Internet traffic represents 50 EXAbytes per year, a fifty-fold increase since 2000. The prefix "exa" stands for one billion billion, or a factor 10^{18}. This amounts to the information contained in 50,000 Libraries of Congress, representing the information in 150 billion books being transmitted every day over the Internet. Another way to look at it is to consider that 10 Tbit/s, the capacity of today's global optical communications, corresponds to the full transmission of 250 digital video-disks (DVD), per second. By year 2009, the optical fibre production and installation produced worldwide was over 160 M km/year. This number converts into 5.2 km/s, fifteen times the speed of sound! By year 2015, at a conservative +17% growth rate, the Earth fibre plant will amount 3 billion kilometres, or over 75,000 times its circumference. It is true that for this generation and others to come, we live in a "connected world". Little known from the vast majority of end-users, the ubiquitous Internet connectivity rests upon this EDFA/WDM web of glass fibres.

The looming issue of a future "bandwidth exhaustion", as described earlier in [6], remains beyond the scope of this article. Here, the idea is rather to provide a flavor of the different technologies being harnessed towards a full exploitation of the currently-available fibre/components bandwidth. Such an activity domain is far to have reached and final conclusion, and this point is important to highlight.

1.2. About this article

This article is a contribution to the celebration of the 50th anniversary of the invention of the LASER, and also a special homage to the 2009 Nobel Prize, Charles K. Kao, for the invention of fibre optics. Our mandate has been to describe, to a broad scientific community, the impact of the LASER in fibre-optics, to highlight the "state of the art" of optical communications, and to share a "view of the future". In 2003 and 2008, similar reviews were published in two previous issues of this journal [8,9]. However, this one is very special, not only due to this celebration context, but also because optical telecommunications seem to have reached an historical turning point, as highlighted above. The task of further describing the scientific and technical issues, and the remaining challenges with respect to *future bandwidth demand*, has been entrusted to five leading contributor teams, covering the following topical areas:

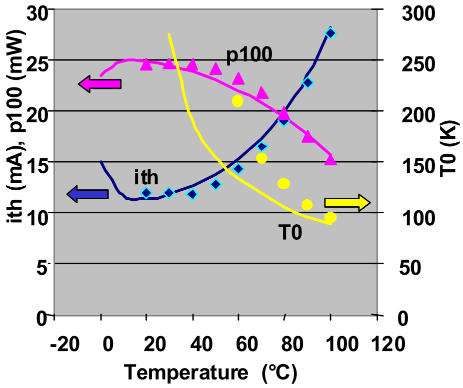

Fig. 3. Self-thermally compensated 10 Gbit/s 1.55 μm laser: Simulated (lines) and experimental (dots) laser threshold, power (at 100 mA) and characteristic temperature T0 for +25 nm DFB detuning.

- *optical components* (by C. Kazmierski et al.), in Section 2;
- *integrated photonic circuits* (by F. Kish et al.), in Section 3;
- *long-haul terabit/s transmission* (by S. Bigo), in Section 4;
- *advanced modulation formats* (by M. Nakazawa) in Section 5;
- *next-generation fibre optics* (by D. Richardson et al.), in Section 6.

Each of these sections are self-introductory and can be read independently, with a concern from the authors to clarify at their best the scientific concepts and the technology challenges, for this journal's readership. A joint conclusion summarises the key issues and questions now facing "modern" optical communications.

2. LASER-based fast photonic sources

2.1. Introduction

Directly modulated Distributed Feed-Back (DFB) single wavelength lasers remain one of the pillars of low-cost transmission equipment for Black&White and Wavelength Division Multiplexing (WDM) applications, owing to their compactness, high output power and low cost. Their fabrication simplicity is a way to further decrease the transmitter cost and to address the new 10 Gbit/s markets of Fibre-To-The-Home access converging with metropolitan networks. An important effort was made recently to increase the operating temperature of DFB in order to decrease, or eventually suppress, thermoelectric cooler consumption in uncooled lowest cost assembling [10] especially for 1.3 μm DFBs, reaching today industrial maturity. However, high temperature 1.55 μm DFBs are also required in order to cover low cost and consumption, large spectral range WDM applications. They are more difficult to obtain due to a larger thermal dependence of material gain at longer wavelengths [11]. Recently, a breakthrough has been attained by the conjunction of high gain AlGaInAs/InP S-QW active material system and strong positive detuning of the DFB peak from the gain peak [12]; this conjunction produces an efficient Self Thermal Compensation of the laser threshold and power. It decreases the power variation at the laser output and allows operating at higher temperatures without changing the bias current (Fig. 3). Such lasers were able to link 25 km standard Single Mode Fibre (SMF) without amplification or dispersion compensation at the industry standard 10 Gbit/s data rate up to 90 °C and 100 km SMF up to 80 °C with the help of electronic equalisation circuits for the first time [12,13]. Further research is now carried out to enhance their speed to 25 Gbit/s and then, maybe, up to 40 Gbit/s.

The speed limits of the directly modulated lasers coming from carrier-photon dynamics can be overcome by an external modulation using material gap modifications induced by a strong electric field. Not involving carriers, electro-optic or electro-absorption modulation effects intrinsically behave with sub-picosecond dynamics. However, the speed of actual components is today technology limited due to their parasitic Resistance*Capacitance (RC) frequency roll-off. They have a special economic interest when integrated with lasers in simple Photonic Integrated Circuits (PIC). While PICs and OEICs (OptoElectronic Integrated Circuits) have been explored for more than 20 years, only a limited number of very simple ones has met any commercial success so far (e.g. wavelength tunable Distributed Bragg Reflector laser, Electroabsorption Modulated Lasers: EML), so that optoelectronic front ends are mainly simple Transmitting or Receiving Optical Sub-Assemblies containing a laser (or electro-optic modulator) or a photo-detector. Recently, by using an enhanced electro-absorption AlGaInAs/InP S-QW active material in a high modulation sensitivity EML PIC, a new step has been reached in terms of speed, with a 60 GHz bandwidth and 86–100 Gbit/s data rate demonstration (Fig. 4) [14]. These results allow energy and cost efficient short-reach and interconnect applications, but also open a way to more complex PICs able to handle much larger data rates due to the very low size (50 μm) of electro-absorption modulators.

Due to the constant telecom traffic increase, a capacity growth by a factor of 30 to 100 will be required by the end of the next decade. Following an evolutionary path based on the simple introduction of additional channels will just not

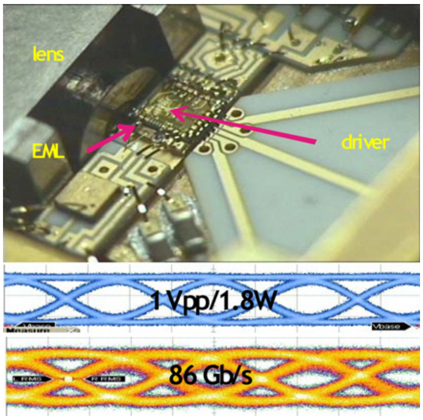

Fig. 4. 86 Gbit/s data rate of a low-voltage InP HBT driver co-packaged with high modulation efficiency EML.

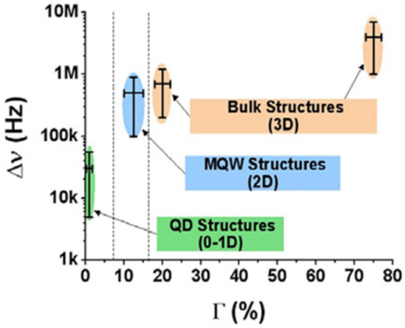

Fig. 5. Evolution of the beating linewidth with the gain confinement factor. The inset shows a comparison of the RF spectrum between a bulk and a QD laser.

bring the appropriate solution [15]. New technological breakthroughs have to be proposed to face this challenge. This is why optical multilevel modulation formats coded in amplitude, phase and polarisation, with both coherent and direct-detection, are presently receiving great attention as a large increase in data rate can be obtained with minimal changes to the installed base of optical filters and chromatic and polarisation mode dispersion mitigation devices. AlGaInAs/InP S-QW laser-modulators-amplifier PICs are showing qualifying performance [16] on the way to cost and energy efficient Terabit/s sources.

2.2. Quantum dot based lasers

Self-assembled semiconductor quantum dot/dash (QD) devices have attracted considerable attention due to their unique energy levels quantification in the three dimensions. QD lasers are expected to present higher performance than quantum well (QW) or bulk based devices, such as lower threshold current, lower chirp and faster dynamic response, able to improve telecom-wavelength laser cost/consumption and to enlarge application fields [17].

However, the most remarkable feature that QDs exhibit up to now is the excellent phase noise of the mode-locked laser (MLL) mode-beating signal. As shown in Fig. 5, the radio-frequency linewidth of the mode beating spectrum is of the order of MHz for lasers with a bulk active layer, several hundreds of kHz for MQW lasers and tens of kHz only for QD lasers [18]. This extremely narrow linewidth for QD lasers is believed to be a consequence of reduced spontaneous emission rate coupled to the lasing mode due to low confinement factor and high four-wave-mixing in these nanostructures. In addition, by optimising both the growth conditions and the design, we developed dots in a well (DWELL) structures very interesting for the generation of high repetition pulses. Indeed, high effective gain can be achieved in these structures, thus allowing one to achieve lasing in short cavity length FP lasers despite the very low optical confinement. As shown in Fig. 6, the use of a 120 μm-long cavity leads to the generation of pulses at a repetition rate of 345 GHz [19].

Owing to this excellent phase noise feature and the large and flat optical spectrum, MLLs can have numerous applications, such as comb generation for wavelength-division-multiplexing (WDM) transmission and millimetre wave (mmW) generation. Indeed, WDM transmission using comb generation in a MLL presents several advantages compared to the use of a set of single mode distributed feedback lasers, since the channel spacing is determined by the MLL mode spacing. Such a WDM channel generation requires only a single Fabry–Pérot (FP) laser and the different channels generated by the MLL are coherent. Once the mode-spacing is matched to the channel spacing, no individual channel frequency control is needed.

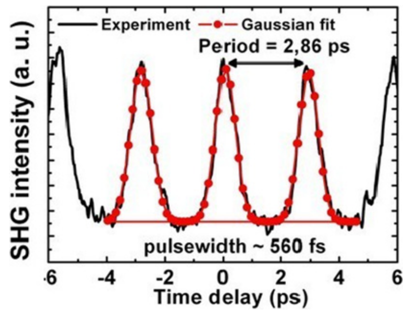

Fig. 6. Optical spectrum (top) and autocorrelation trace (bottom) for 120 μm-long QD laser demonstrating a repetition rate of 345 GHz.

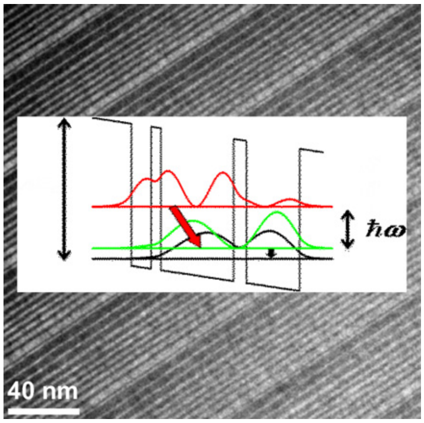

Fig. 7. Transmission Electron Microscopy image of a QCL structure. Insert: Typical conduction band diagram of a QCL.

We demonstrated recently the comb generation in the 1.5 μm window and error-free transmission over 50 km SMF of 8 WDM ITU channels at 10 Gbit/s with a channel spacing of 100 GHz for WDM transmission in a QD-MLL [20]. Owing to the reasonable relative intensity noise level, a penalty of only 1.5 dB is achieved compared to the use of an external cavity CW laser. Such a good performance allows one to consider such a solution in an integrated WDM transceiver. The very low radio-frequency linewidth of QD-MLLs makes these devices very attractive for high frequency signal generation for radio transmission or radar applications [21,22]. As an illustration, we have integrated the 54.8 GHz MLL into a dual loop coupled optoelectronic oscillator using suitable fibre length values. The phase-noise reduction is more than 30 dB at an offset frequency of 50 kHz giving a phase noise below −82 dBc/Hz, at this offset frequency. Moreover, we demonstrated that the generated 60 GHz waves using a QD-MLL can be successfully used for wireless transmission through external modulation or direct modulation. For instance, a frequency up-conversion from 6 GHz to 60 GHz of an OFDM signal was realised by directly modulating a FP MLL whose mode-beating frequency is 54 GHz. This results in a simple up-conversion scheme with improved conversion efficiency; it also provides means to transport and to distribute the 60 GHz radio signal using radio-over-fibre transmission.

Such a remarkable performance paves the way for the penetration of QD technology into the ICT market. Further material optimisation are still on-going in order, for instance, to reduce the inhomogeneous broadening and the polarisation sensitivity of QDs, which result from their strain-driven nucleation process, and to identify the more relevant telecom applications for such nanostructures based devices.

2.3. Quantum cascade lasers

The quest to produce powerful light sources covering the Mid-Infra Red (Mid-IR) 3–12 μm wavelength range for defence, security and environmental applications is still very strong. Several technological options are today available or under development. Among the technologies available, semiconductor sources appear to be the best long-term option since they are involving only one electrical-optical conversion that can be very efficient. Furthermore, semiconductor lasers have a potential for extreme compactness, high lifetime, high reliability and low cost. Quantum Cascade Lasers (QCLs) are today the only semiconductor laser sources operating at room temperature in pulsed or continuous modes over the 4–10 μm wavelength range.

The quantum cascade laser is a semiconductor light source based on resonant tunnelling and optical transitions between quantised conduction band states [23], see Fig. 7. Instead of being classically fixed by the physical properties of the constituent materials, the lasing mechanism mainly depends on the layer sequence forming the heterostructure, giving a unique

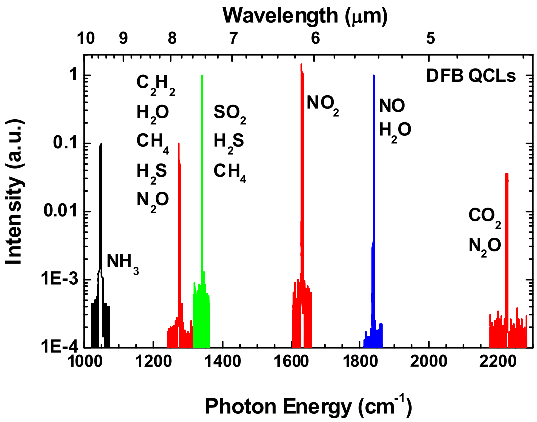

Fig. 8. DFB QCL spectra of devices available at Alcatel-Thales III-V Lab. The corresponding molecules for gas sensing applications are indicated.

flexibility for designing devices emitting in a wide spectral range up to the THz region (3.5–160 μm). At present, the best performance is reached at wavelengths between 4–10 μm.

Two main QCL families can be defined, according to their applications: high power Mid-IR QCLs for Optical Counter Measure (OCM) for sensor jamming or dazzling and tunable single mode Mid-IR QCLs for explosives, drugs, Chemical Weapon Agents (CWAs), see Fig. 8, Toxic Industrial Chemicals (TICs) and pollutant agent spectroscopy. Free-space optical communications could be a possible application which will also take advantage of the Mid-IR atmospheric transparency windows.

QCLs were invented 15 years ago and have now reached a certain degree of maturity. However, the business of quantum cascade lasers is still in its infancy. There are today only two commercial companies in Europe which are really able to fabricate and deliver quantum cascade lasers: a Swiss SME called Alpes Laser founded in 1998 by Jérôme Faist, one of the co-inventors of QCLs and Alcatel-Thales III-V Lab.

Single-frequency operation of the laser is required for spectroscopy application. It is usually achieved by introducing a distributed feedback (DFB) structure into the QCL active region in order to favour a particular mode. Pulsed mode operation of these devices at Room Temperature (RT), mounted on a Thermal Electric Cooler (TEC) is now easily achieved. On the other hand, Continuous Wave (CW) RT operation lasers on TEC are still more lab devices than commercial products [24]. Fabry–Pérot QCLs operating in CW at RT in the 4–5 μm range with an output power of 500 mW and a beam quality factor of $M^2 \sim 1.2$ (diffraction limited) in the fast and slow axes are currently available to be evaluated in systems for protecting aircrafts from shoulder-fired missiles. Maximum single-ended continuous-wave optical power levels of 3 W at 4.6 μm at RT were obtained recently by US labs. This power level corresponds to maximum wall plug efficiency (WPE) of 13% for a multi-mode transverse beam [25].

The main limiting point to reach today high-power quantum cascade laser sources is their low WPE which is currently investigated by several research groups. The theoretical limit ($\sim 30\%$) is an open problem, but it exceeds by far the currently achieved world record ($\sim 16\%$) and commercial device performance ($\sim 5\%$). Besides the improvement of the intrinsic performances of the single QCL element, integrated chip-level approaches will constitute the innovative solutions for the foreseen applications. As an example, the hybrid evanescent-wave integration of QCL on silicon (or Ge/Si) waveguides is a promising technique to demonstrate infrared spectrometer-on-a-chip [26]. Concerning a future DIRCM system where cost and power scaling will be important, an extraordinarily high power beam with a single transverse mode could be obtained by beam combining of several phase locked QCLs on the same chip.

Although the main applications of QCLs are focusing today on chemical detection and sensor jamming, their physical properties are very attractive for long-term evolutionary step in energy efficient telecommunications with growing speed and capacity requirements. For example, QCLs may solve spectral overcrowd in wireless communications, potentially providing terahertz bandwidth and energy efficiency improvement due to directional targeting of reduced size cells. Also, the progress of new materials such as GaN and related compounds may bring a revolution in fibre telecom laser speed working at 1.3–1.5 μm, no longer limited by photon–electron resonance [27].

2.4. Photo-detectors

Imaging, photovoltaics and optical fibre transmission have been the main drivers in the evolution of photo-detectors during the last decades, in particular in the visible and near infrared part of the spectrum. In the area of optical fibre transmission, this evolution followed three main directions, while keeping the conversion quantum efficiency close to one:

– increase of the wavelength of interest, from 0.85 μm to 1.5 μm;
– tremendous increase in the data rates;
– improvement in sensitivity.

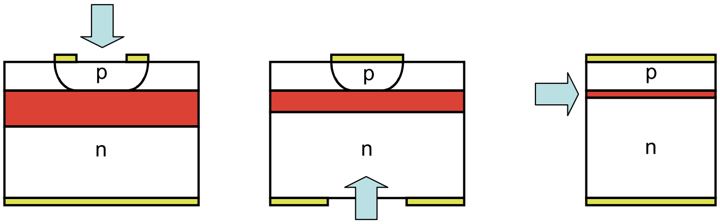

Fig. 9. Evolution of InGaAs/InP photo-diode structures towards thinner absorption region, and increased bandwidth, from the front illumination scheme (left) to back illumination (middle) and finally side illumination (right). Simultaneous reduction of the junction area results in lower junction capacitance, and overall larger optoelectronic bandwidth.

One family of photo-detectors established itself as the most efficient one: the pn or pin photo-diode, in which the absorption region is mainly located in the junction depletion region where the high electric field separates photo-carriers. While the first photo-diodes for telecom were made in silicon, providing good absorption at 0.85 μm wavelength, a compound semiconductor, InGaAs, lattice-matched to InP was used for the longer wavelengths: owing to its absorption characteristics, since this material provides excellent responsivity up to 1.6 μm wavelength, together with a large bandwidth resulting from the short associated absorption length (1 to 2 μm).

As the bandwidth requested by growing data rates was increasing, the photo-diode structure itself kept evolving thanks in particular to the use of heterojunctions:

– at first, transparency of the InP substrate (and of the front p-layer) was instrumental in allowing a back illumination scheme rather than the conventional front illumination. This new scheme allowed one to reduce the InGaAs absorption layer thickness by a factor of two, while reducing simultaneously the junction area (both transit time and charging time are then lowered);
– a second major step is associated with the double heterostructure scheme [28], similar to a semiconductor laser, with a very thin absorbing core (very short transit time) compatible with very large optoelectronic bandwidths ($>$100 GHz). Reaching a good coupling efficiency between the cleaved or lensed fibre and the photo-diode required an important development. Edge illuminated photo-diodes are now available, with a large acceptance input multi-mode waveguide and an evanescently coupled thin absorption junction [29,30]. Such photo-diodes offer a figure of merit (bandwidth $\times$ responsivity) of 50 GHz A/W at 1.5 μm (see Fig. 9).

After propagation, the optical signal power is most often quite weak, and can hardly be separated from noise. In order to increase the sensitivity, several solutions have been investigated: (i) integration with high sensitivity electronic amplifiers, such as the Transimpedance Amplifiers (TIAs); this actually motivated many developments in the area of Optoelectronic Integrated Circuits (OEICs); (ii) association with optical pre-amplifiers; this technique is widely used in WDM receivers in which several photo-receivers can share a same pre-amplifier; (iii) avalanche photo-detector with internal photo-current multiplication. In this device, impact ionisation is activated by applying a large electric field. Through this process, photo-carriers are multiplied and the output signal as well. First avalanche photo-diodes (APDs), made from silicon, exhibited almost ideal characteristics: bandwidth of a few hundreds MHz, large enough for the intended data rates (34–140 Mb/s), useful avalanche gain of about 100 without bandwidth reduction, and low excess noise. Such characteristics, resulting from the very attractive ionisation properties of Si and from a structure design fully benefiting from these properties (the so-called $p\pi p\pi n$ structure), have not been met with materials suited for longer wavelengths, whether Ge or InP related compounds. However, high performance APDs have been fabricated in this latter material system, owing to two main innovations:

– a design suited to avalanche operation, with Separate Absorption Grading and Multiplication regions (SAGM): while absorption occurs in InGaAs, multiplication takes place in a wider bandgap, and lower dark current, material; an intermediate region, providing some bandgap grading, prevents carriers trapping;
– an avalanche material with acceptable properties. InP was the choice material for the first APDs. However its poor ionisation characteristics resulted in a factor of merit (gain $\times$ bandwidth) of 60–80 GHz, too low for 10 Gbit/s applications. With a more favourable ionisation coefficients ratio and a factor of merit in the 140–160 GHz, AlInAs offered an acceptable solution for these data rates, providing a sensitivity close to -30 dBm at 10 Gbit/s [31].

Photo-detectors keep evolving, adjusting to the market needs. For instance, the trend in long haul transmission is to rely on spectrally efficient modulation schemes, possibly with coherent detection. Such schemes require large bandwidth, high linearity photo-diodes, a challenge for photo-diodes with a decreasing active region and higher associated carrier density. Power consumption in routers and switches is also a problem, which can benefit from an improved photo-receiver sensitivity, a challenge for OptoElectronic Integration, whether on InP or Si.

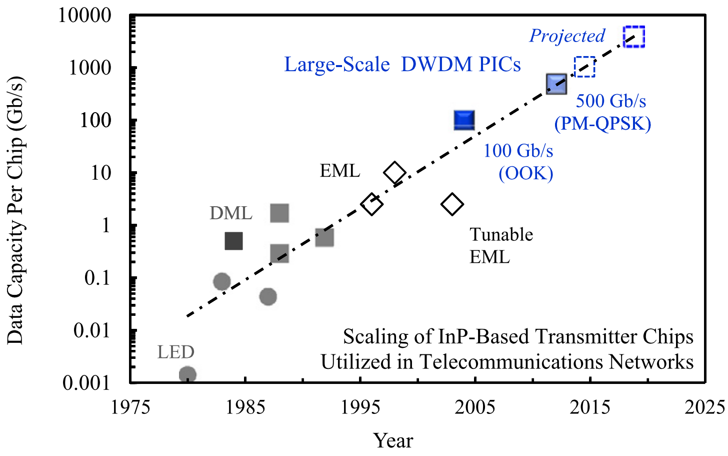

Fig. 10. Scaling of the data capacity/chip for InP-based transmitter chips utilised in commercial telecommunications networks. All data points are for deployed commercial networks except the 500 Gbit/s chip that is in development.

2.5. Conclusions

Discrete or small-scale PIC transmitting and receiving components, especially those based on indium phosphide technology, have become an integrated part of the optical fibre communication industry. The unique ability of the InP materials family to efficiently generate laser emission in silica fibre transmission windows makes the associated technology the best candidate for larger scale integration of all optical functions. However, improvement of discrete component characteristics for higher performance in speed, chip size, electro-optical conversion efficiency and high temperature operation remains a major quest. In the coming decade these devices will be facing the challenge of supporting a growing transmission capacity demand, while offering the increased requested wavelength agility and, simultaneously, a low environmental cost (low energy and material consumptions).

InP-laser based technical progress increasingly coincides with a larger societal impact: from connecting people, this technology now addresses emerging applications and markets like security, medical imaging, pollution sensing, etc. One would see there a seed for next technological revolutions better accounting for limited Earth's resource constraints.

3. Monolithic LASER integration into large-scale photonic circuits

3.1. Introduction

The discovery of the laser 50 years ago [32] was followed two years later by the realisation of a semiconductor version [33–36], despite the fact that considerable new physics were needed to be discovered to realise this form of laser (using p–n junctions to inject current in a direct gap semiconductor to obtain stimulated emission). Since its discovery, the semiconductor laser has made tremendous advances, including (but not limited to) the development of: heterojunction lasers and cw operation [37,38], the realisation quantum-well lasers [39], and the development of distributed feedback (DFB) lasers [40,41]. This progression, combined with the development of long-wavelength InP-based semiconductor lasers in the low-loss spectrum of the optical fibre [42], enabled the deployment of semiconductor lasers to enable transmission in optical fibre networks.

Since the first laser was deployed an optical fibre network in 1984, there has been a steady scaling of increased capacity per chip as shown in Fig. 10. Discrete devices (first LEDs and later directly modulated lasers (DMLs)) were deployed during the first ~ 15 years of building optical networks. In order to continue to scale both the data capacity and performance, the development of photonic integrated circuits (PICs) was required [43]. The first transmitter devices deployed in optical fibre networks began with small-scale integration and consisted of electroabsorption modulated lasers [44]. This enabled the realisation of devices with a capacity up to 10 Gbit/s per chip. The next significant progression occurred with the development of large-scale PICs where over 50 devices were integrated onto a monolithic chip to realise a 100 Gbit/s transmitter chip (10 channels $\times$ 10 Gbit/s) [45]. This advance represented an order of magnitude increase in data capacity per chip compared to existing commercial devices and utilised a multi-wavelength array of ten tunable DFB lasers (aligned to an ITU grid). Next generation large-scale PIC technologies (not yet deployed) are being developed with capacities of $\geqslant$ 500 Gbit/s (5 $\times$ 100 Gbit/s and above [46]), and integrate over 400 functions onto a single chip.

The scaling of electronic integrated circuits has progressed at an exponential rate as predicted by Moore [47] since their invention in 1959 [48,49]. This is in contrast to photonic integrated circuits, where the pace of integration has been dwarfed relative to electronic ICs. This dramatic difference is mainly due to the inability of the value delivered by a PIC to outweigh the cost of integrating optical elements monolithically onto a chip.

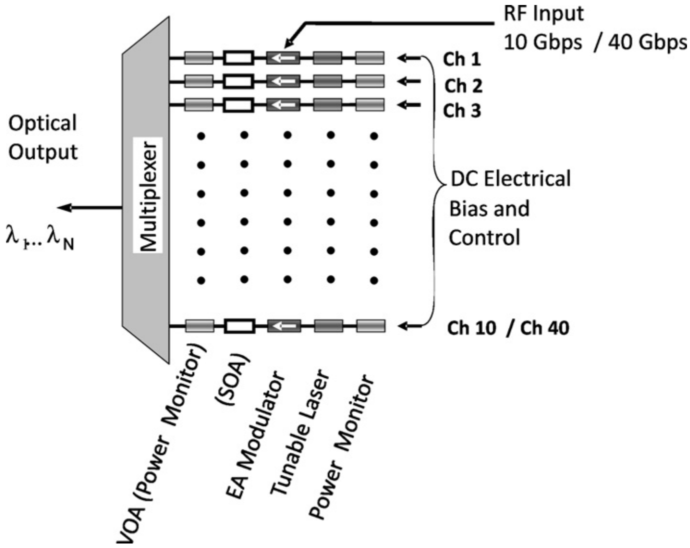

Fig. 11. Schematic of the OOK large-scale PIC transmitter chip. The commercially deployed devices have 10 channels whereas 40 channels have been demonstrated on research devices. The SOA elements on the second generation chip enable the PICs to be capable of being deployed in ULH and submarine applications.

Circa 2001, numerous developments in the III-V semiconductor and optoelectronics field corroborated to help enable the development of commercial large-scale photonic integrated circuits. These included the development of high-quality, low-defect density 50–100 mm diameter InP substrates, the development of metal-organic chemical vapour deposition (MOCVD) as a viable means for the growth of high-precision lasers and optoelectronics devices, the development of precision dry-etch technologies for low-loss waveguides and reliable devices, and fine line lithography. This "tool kit" allowed the construction of a PIC fabrication capability that was designed from the outset for manufacturability. Large-scale PICs could then be developed in such a facility using a similar methodology as electronic ICs, wherein designers are given a fixed (limited) tool set (e.g., design rules) to design within, resulting in a manufacturable (cost-effective) device. This methodology was used at Infinera Corporation, simultaneously combining the large-scale PIC capability with the design and development of network products that maximised the value delivered by large-scale PICs. This provided, for the first time, a viable commercial source and value proposition for such devices.

3.2. 100 Gbit/s transmitter PICs

A schematic diagram of the architecture of commercial large-scale transmitter PICs is shown in Fig. 11. These devices consist of a 10-channel array with each channel consisting of tunable laser integrated with an electroabsorption (EA) modulator, a variable optical attenuator (VOA), and a power monitor. Each of the 10 channels is then multiplexed into a monolithically integrated arrayed waveguide grating (AWG) which provides a single output for fibre-coupling in a hermetic package. The devices are hybrid packaged with a 10-channel analog ASIC EA modulator driver chip and are Telecordia qualified to GR-468 standards. A second generation 100 Gbit/s large-scale PIC transmitter capable of ultra long-haul/submarine reaches ($>$ 600 km) [50,51] has been also developed and deployed which adds per-channel semiconductor optical amplifiers and substitutes power monitors for the VOAs.

The 100 Gbit/s transmitter PICs consists of 10 channels arranged on a 200 GHz grid in the C-band (the system performs downstream multiplexing of similar transmitters to achieve a system-level 25 GHz grid). The spectrum of the lasers from such a transmitter PIC is shown in Fig. 12. The lasers are tuned to within $< \pm 2$ GHz of the ITU grid over life and exhibit an SMSR $>$ 40 dB. In addition, superimposed on the laser spectra of Fig. 12 is the AWG multiplexer transmission function. This shows that the AWG pass-bands and laser frequencies are very well-aligned, resulting in minimal power loss from misalignment.

Large-scale 100 Gbit/s PIC transmitters were first commercially deployed in 2004, with devices now operating for over 46,000 hours in the field Over 400 M field hours have been accumulated on commercially deployed devices (PIC Transmitter modules) corresponding to $<$ 2.5 FIT, which is comparable to the discrete pump lasers [52], albeit on PICs with over 50 monolithically integrated elements.

3.3. 500 Gbit/s coherent transmitter PICs

The large-scale PIC transmitter platform has shown to be capable of scaling beyond the currently deployed commercial 100 Gbit/s devices. Specifically, devices have been demonstrated extended the channel count of the commercial devices

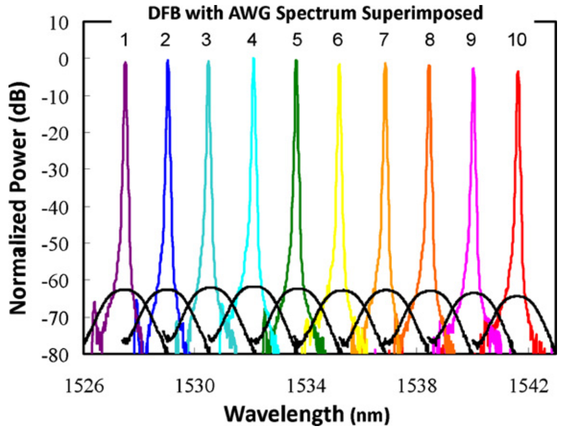

Fig. 12. Superposition of the 10 channel DFB spectrum with the AWG multiplexer transmission function for 10-channel large-scale PIC transmitter.

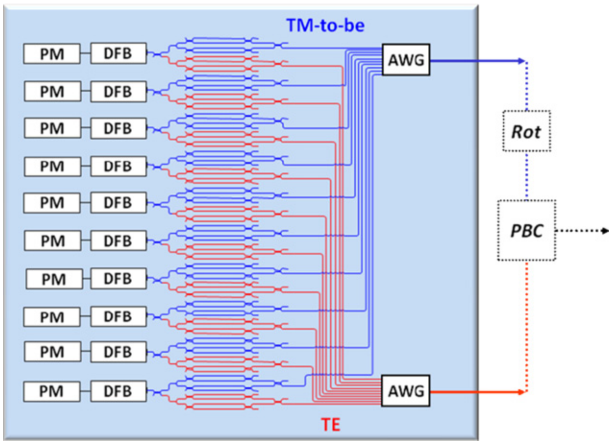

Fig. 13. Schematic of the 10-channel, 500 Gbit/s pol-mixed QPK transmitter PIC. All elements are monolithically integrated on a single chip except the polarisation rotator (Rot) and beam combiner PBC which are off-chip.

(in Fig. 10) to 40 channels as well as simultaneously increasing the speed of the EA modulators from 10 Gbit/s [53] to 40 Gbit/s [54] with $>$ 200 elements integrated on single chip.

For bit rates beyond 10 Gbit/s, phase-based modulation formats offer distinct advantages in link and network performance, including 2–4$\times$ gains in spectral efficiency and better optical signal-to-noise ratio (OSNR) tolerance [55]. High-capacity large-scale PIC transmitters capable of polarisation-multiplexed quadrature phase-shift keying PM-QPSK at 400 Gbit/s and 500 Gbit/s have been developed [46,55,56]. A schematic of such a chip which integrates over 400 elements per chip is shown in Fig. 13. The device consists of 5 channels, operating at 100 Gbit/s channel where each channel consists of 2 carriers (wavelengths) [56]. This dual-carrier format has been shown to enable superior performance at lower baud rates than a single-carrier (wavelength approach) [57]. Each channel consists of a DFB (with back power monitor) which feeds two distinct nested I-Q Mach–Zehnder modulators that are then multiplexed into two distinct AWGs. The output from one of the AWGs is polarisation rotated (off-chip) and then combined (off-chip) with the other output to produce a polarisation-multiplexed architecture.

Fig. 14 shows the exemplary constellation diagram for one of the 10 carriers that are output from the 500 Gbit/s transmitter PIC in a packaged module. The input data streams are generated using two independent but synchronised pattern generators operating at 14.25 Gbit/s, with the input data consisting of two delayed PRBS $2^{15}-1$ patterns. The output of the transmitter PIC is characterised using a custom coherent receiver which includes a 50 Gs/s high-speed realtime sampling scope and proprietary signal processing. The other carriers operate with similar performance across the entire PIC.

Laser linewidth (phase noise) is a critical parameter for the successful high-performance operation of phase-modulated systems and PICs. Accordingly, we have developed lasers with narrow linewidth integrated into the phase-modulated PICs. An example of the power spectral density (PSD) of a laser fabricated on the same wafer as the 500 Gbit/s transmitter PIC is shown in Fig. 15 [58]. The inferred laser linewidth from this data is $\sim$300 KHz and is sufficient for meeting the performance required of long-haul and submarine networks for 500 Gbit/s PIC applications.

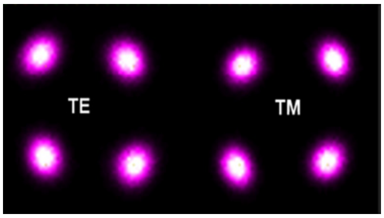

Fig. 14. Dual polarisation 14.25 Gbaud constellation diagrams for one carrier of a 500 Gbit/s PM-QPSK transmitter PIC.

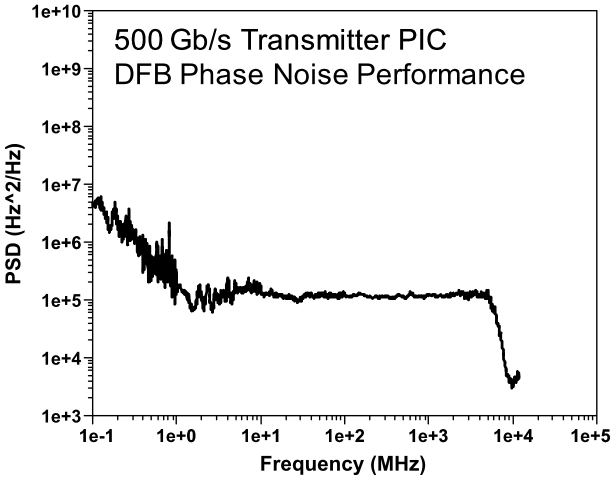

Fig. 15. Single-side power spectral density (PSD) of a DFB laser from a test chip that is simultaneously fabricated on the same wafer as the 500 Gbit/s QPSK transmitter PICs [56].

3.4. Conclusions

After 50 years, the utility of the laser continues to thrive and prosper. The semiconductor laser is no exception. In optical communication applications, the semiconductor laser is a key enabling technology of the "optical engines" that power the network. The continued scaling of the network, and the "optical engines" that drive it will be essential to continuing to cultivate the communication revolution. Large-scale photonic integrated circuits utilising arrays of semiconductor lasers have been developed to address this need and are one of the most promising technologies to assure it's continued scaling.

4. Petabit transmission systems and technologies

4.1. Introduction

The backbone network is where inter-city or inter-continental communications take place. It encompasses the most demanding fibre routes, sometimes of multi-terabit/s capacity [59]. Along all these routes, light carries data using the wavelength division multiplexing (WDM) technique. Several semi-conductor laser light sources, up to typically one hundred, each at a different wavelength, carry a fraction of the total binary data stream, 10 Gbit/s, 40 Gbit/s or soon 100 Gbit/s. They are generally combined and separated using optical gratings, and travel altogether across the fibre links. Their output power is relatively moderate (in the range of 10 mW) and they are reamplified every 50–100 km by optical repeaters, essentially based on erbium-doped fibre amplifiers (EFDA). EDFAs are fed with semi-conductor laser light as well, generally at 980 nm wavelength, but at higher powers (100–300 mW). We discuss next the technologies which have been proposed to carry the largest capacities over very long transmission distances and discuss some research challenges ahead of us in optical networks. We use the recently reported record 112 Petabit/s km experiment [60] as an example.

4.2. Packing more information into the available optical bandwidth

In Wavelength-Division Multiplexed (WDM) optical systems, the system capacity is equal to the number N of carrier wavelengths, times the bit-rate B carried by each of them. In a given wavelength range (manageable by the optical amplifiers), increasing capacity in a single fibre can be obtained by two approaches, i.e. by increasing N while packing wavelengths closer, and/or by increasing B. Both amount to increase the bit-rate per available unit frequency, also known as the information spectral density (ISD). Today the ISD reaches at best 80% (or 0.8 bit/s/Hz). As the information spectral density is increased, the carrier wavelengths suffer from stronger cross-talk from their closest carrier neighbours, either when

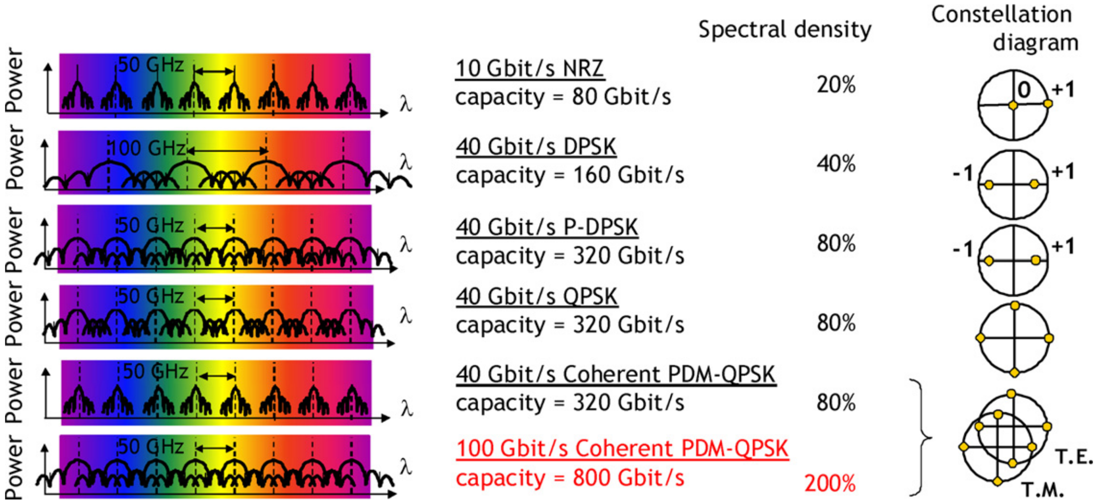

Fig. 16. Computed optical spectra (all at same scale) showing various approaches to fill an amplifier bandwidth. The constellation diagram depicts the possible modulation states taken by the complex electric field of light at the same energy per bit for all diagrams.

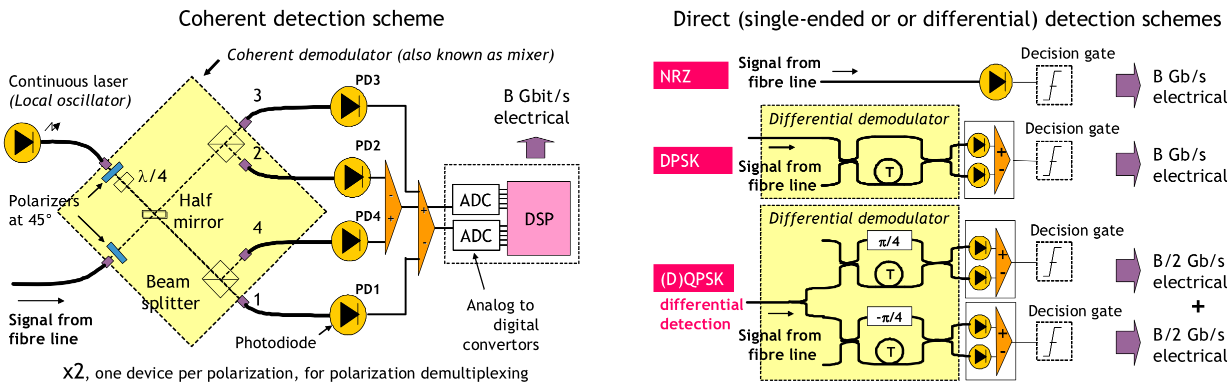

Fig. 17. Schematic of a coherent-detection receiver (left), as compared to direct-detection receivers (right)

multiplexing (combining carrier wavelengths) or demultiplexing (separating carrier wavelengths), or during fibre propagation, unless disruptive approaches are used. Coherent optical solutions have now been adopted as the most promising. These solutions are just starting to provoke to a radical change in the design of optical networks, with possible implications as vast as that following the introduction of the EDFA in the 1990s.

Containing the spectral width of each wavelength carrier is the most straightforward remedy against increasing cross-talk. For each carrier, the incoming bits are encoded into a stream of successive symbols, at a rate called symbol rate. In today's optical systems, symbols can take only two states, e.g. "1" or "0", and hence the symbol rate matches the bit-rate, the symbols are encoded by varying the intensity of light (light ON or light OFF) according to the widespread non-return to zero (NRZ) format, or by varying the phase (0 or π) according to the differential Phase-Shift Keying format. However, the spectral width about each wavelength carrier is approximately twice the symbol rate (e.g. 80 GHz at 40 GSymbol/s). It can be truncated with a narrow optical filter [61] as with Partial-DPSK (PDPSK) [62], but to some extent only. A more efficient way for increasing the bit-rate per carrier wavelength, without affecting the spectral width, is to increase the possible number of modulation states per symbols beyond two (see Fig. 16). One of the most interesting modulation formats would consist in allowing symbols to take four phase states, to make Quadrature Phase-Shift Keying (QPSK). By employing polarisation division multiplexing (PDM), i.e. by encoding two different QPSK data streams along the two polarisation components of light, a bit rate per carrier wavelength four times as large as with two states per symbol can be obtained over unchanged spectral bandwidth. This has opened the way to carrier wavelengths modulated at 100 Gbit/s (25 GSymbol/s) over the same 50 GHz frequency grid as at 10 Gbit/s, but with tenfold increase of information density at 200% (2 bit/s/Hz).

4.3. Coherent detection

Recovering the signal multiple symbol states is the challenge that a coherent receiver can solve. Such a receiver is inherently more complex than conventional direct-detection (see Fig. 17). The contrast is naturally greater when compared

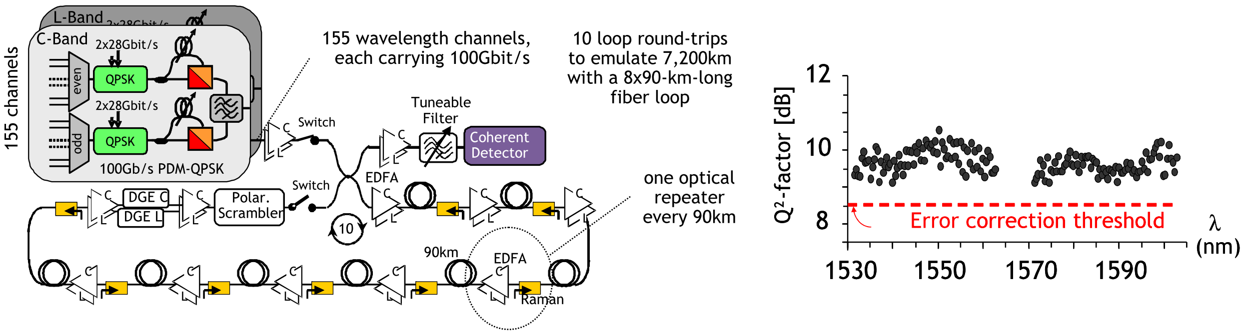

Fig. 18. Schematic of 112 Petabit/s km experiment (left) Q^2 factors of the 155 WDM channels (right).

with receivers for NRZ, than with receivers involving differential detection for Phase-Shift Keyed formats like DPSK and Differential QPSK. Coherent detection relies on the beating onto photo-diodes of the signal beam with the beam of a cw laser called the local oscillator, normally a twin of the signal laser used to generate the optical data at the transmitter. Both beams are combined into a coherent mixer, which generates four interference beams from the four output ports. The mixer is designed such that, from one port to the next, the relative phase between signal and local oscillator has been rotated by another 90°. Ports 1 & 3 and 2 & 4 are feeding two sets of balanced photo-diodes (Fig. 17). To achieve polarisation demultiplexing, two coherent mixers should be operated in parallel. Their photo-currents are sampled before further digital processing. In contrast to conventional photo-receivers for NRZ format which only provide the signal power out of a simple photo-diode, coherent receivers provide the signal amplitude, phase, and state of polarisation.

Powerful algorithms convert the digitised waveforms from the four photo-diodes back to bit streams. Additionally, the availability of the full signal characteristics opens tremendous opportunities against all the impairments that limit the achievable transmission distance in today's fibre systems. The tolerance to noise, to Polarisation Mode Dispersion [63], to chromatic dispersion [59], and to a large cascade of reconfigurable nodes distributed along the link has already been extended to ranges unseen with other techniques. However, the algorithms must process a very high flow of data in real time, e.g. 1 Terabit/s per chip. Challenging though the implementation seems, coherent detection has already been experimented in commercial product for 100 Gbit/s applications since mid-2010.

In the experiment described next, the chip is emulated with a free-running oscilloscope, while the Analog-to-Digital Converters (ADC) of Fig. 17, right, are replaced by its sampling heads. This oscilloscope operates at a rate of 50 GSamples/s and can store 0.5 million samples at once, simultaneously from all four heads. These samples are used to convert optical data back to electrical data streams with digital signal processing in successive steps: re-sampling at twice the symbol rate, possible dispersion compensation through Finite Impulse Response (FIR) filter, digital clock recovery, polarisation demultiplexing through 5-tap adaptive filtering based on the Constant Modulus Algorithm (CMA) [64], carrier-phase estimation using the Viterbi and Viterbi algorithm [65] and finally symbol identification. After symbol identification, the received electrical bit streams are compared to the original from the transmitter for error counting.

4.4. 112 Petabit/s km experiment

Recent research has shown that the full potential of coherent detection can only be revealed with its association with alternative technologies, not used in today's 10 Gbit/s networks. The aforementioned multi-level modulation formats and PDM are two technologies which belong to this category. We shall now use the example of the first experiment with a capacity times distance product in excess of 100 Petabit/s km [60], to discuss other technologies that hold big promises when associated with coherent detection. In this experiment 155 lasers are modulated at 100 Gbit/s and transmitted over 7200 km, as when 400 DVDs per second need to be sent across the ocean via a single optical fibre.

The transmitter is schematized in Fig. 18. It involves 155 distributed feedback (DFB) lasers spaced by 50 GHz, ranging from 1531.51 nm to 1562.64 nm in the C-band and from 1571.24 nm to 1602.74 nm in the L-band. The even and odd channels of each band are combined into two spectrally-interleaved wavelength combs. Both combs are modulated independently into separate QPSK modulators, fed with 2^{15} 1 bit-long sequences at 28 Gbit/s, emulating 7% Forward-Error Correction (FEC) and protocol overheads. The output from each modulator is split along two polarisation-maintaining fibre (PMF) paths in a 3 dB coupler. The QPSK data along one path are delayed by hundreds of symbols into a PMF, before being polarisation-multiplexed with the QPSK data along the other path through a polarisation beam combiner. This scheme produces PDM-QPSK channels at 112 Gbit/s. The odd and even channels are then spectrally interleaved through a 50 GHz interleaver, and boosted into a C-band or an L-band EDFA, whichever applies. The output of C and L EDFA boosters are combined thanks to a C/L multiplexer and injected into the recirculating loop. The loop consists of eight 90-km-long spans of Enhanced Pure Silica Core Fibre (E-PSCF), characterised by 110 μm^2 effective area, 0.168 dB/km average loss, < 0.1 ps/$\sqrt{km}$ polarisation mode dispersion. No dispersion-compensating fibre is used here, in contrast to all experiments performed at 10 Gbit/s. Fibre loss is compensated for by hybrid Raman–erbium optical repeaters. Each repeater incorporates a C-band

EDFA and an L-band EDFA, operating in parallel, and a Raman pre-amplifier. The pre-amplifier is designed to provide ∼10 dB on-off gain, thanks to backward-propagating laser diodes at wavelengths 1432 nm, 1457 nm and 1487 nm. It is spliced to the set of EDFAs. Further power adjustment is performed thanks to a couple of dynamic gain equalisers (DGE), inserted at the end of the recirculating loop. The loop is filled and emptied thanks to two acousto-optic switches, triggered by time-delay generators, synchronously with the bit-error rate (BER) test equipment.

At the receiver end, each channel can be isolated from the rest of the multiplex by a tunable filter, and is sent to the coherent receiver of Fig. 17, right. The optical data streams make ten loop round-trips, i.e. 7200 km, before exiting for bit error counting. No more than 1 error out of 10^{12} transmitted bits is required after forward error correction (FEC). This condition amounts to requiring that the Q^2 factors should remain greater than 8.5 dB (corresponding to an uncorrected BER of 4. 10-3). Four sets of 2 million samples are used here to calculate the error ratios at all 155 wavelengths. They are converted into Q^2 factors and depicted in Fig. 18, right, versus wavelength. The average Q^2 factor is 9.7 dB, while the min Q^2-factor is never lower than 9.1 dB. This experiment sets an important milestone by breaking the capacity × distance barrier of 100 Petabit/s km, largely thanks to coherent technologies. As such, it paves the way for future bandwidth expansions.

We shall now discuss some of the research challenges that lay ahead of us when a WDM optical fibre link such as described above (based on coherent technologies or not) is inserted into an optical network.

4.5. More transparent optical networks

Optical networks consist of nodes, preferably located in densely populated areas, connected by fibre links. Today, they are still largely opaque, which means once the data stream has been converted to an optical stream by the input node, it experiences successive optical-to-electrical and electrical to optical conversions at any intermediate node before its destination node is reached. By contrast, in transparent networks, the optical data stream can travel across all intermediate nodes without conversion to electronics [66]. Ideally, the transparent intermediate nodes can be reconfigured and as such, become optical cross-connects. Numerous challenges remain to be solved in order to create fully meshed optically transparent networks. For example, longer distances will need to be bridged, over a greater variety of fibre types than today's [67]. The interactions between signals at various bit-rates, will cause new propagation impairments (nonlinear effects, primarily) that have to be contained. In order to contain the above spurious effects, coherent detection and massive digital signal processing will most likely be very helpful. Transparency has the additional advantage of contributing to more energy-efficient networking without decreasing flexibility. In summary, optical transparency is a useful approach for decreasing cost (cost/bit) and energy consumption (J/bit).

4.6. More dynamic optical networks

The increasing competition on leased-lines and virtual private network services strongly encourages operators to offer quicker allocation of bandwidth between users [68]. Making optical networks dynamic means controlling and managing connections remotely and automatically. The introduction of optical cross-connects in the nodes is one of the first requirements for transport network dynamicity. But dynamicity also requires a control software (or plane) of the network. In each node, it should drive the configuration of the optical cross-connects (which wavelength from an input fibre goes to which output fibre), but also force electronic regeneration of some wavelengths, that cannot be sent transparently all the way to their destinations. This software has to be impairment-aware, i.e. aware of the feasibility of all optical paths before establishing connections [67]: this is, by itself, a real challenge. In the routing process of optical channels, the control plane will also have to take into account energy consumption, thus allowing energy-aware optical networking. The motivations for dynamicity can be partly addressed by remote wavelength management, thanks to cross-connects. However, other approaches deserve to be investigated as a complement or to go beyond. The most promising of them consist in automatically varying the bit-rate per wavelength, continuously or step-wise, or in varying the wavelength spacing. Other strategies rely on optical switching with much finer granularity than the optical wavelength channel, whether at burst or packet level. These optical burst or packet switching techniques allow efficient aggregation of traffic coming from access networks, and will spread into metropolitan networks first, then into backbone networks.

4.7. Conclusions

The revival of coherent detection, paired with digital signal processing, polarisation multiplexing and multi-level modulation formats has created a new momentum in high speed fibre links. There is little doubt that this momentum will drive research to transmission achievements beyond the current, aforementioned record of 112 Petabit/s km soon. It will also have an impact on the design of the full optical networks where the high-speed belong, while allowing one to meet the growing demand for optical transparency and dynamic.

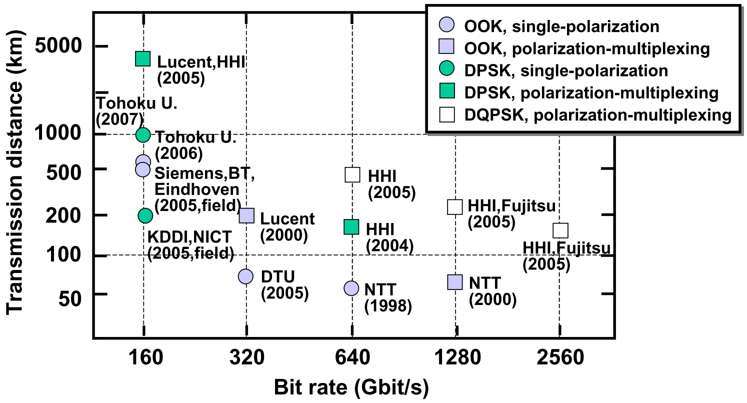

Fig. 19. Recent experimental demonstrations on ultrahigh-speed OTDM transmission.

5. New frontiers in optical communications through multi-level coherent transmission

5.1. Introduction

To cope with the rapid growth of Internet traffic on a global scale, intensive efforts have been made to expand the capacity of optical backbone networks. Recent trends in optical communication research can be divided mainly into two categories. One is ultrahigh-speed transmission using ultrashort pulses, in which optical time division multiplexing (OTDM) is adopted to increase the bit rate per wavelength channel that exceeds the limit of electrical signal processing [69]. This is the driving force behind attempts to realise an ultrahigh-speed optical network with a simple configuration, large flexibility, and low power consumption, in which the complexity of wavelength routing at the switching nodes can be alleviated through the need for fewer wavelength channels. The other trend is ultrahigh spectral density coherent transmission employing multi-level modulation formats, whose aim is to expand the capacity of WDM transmission systems within a finite transmission bandwidth [70,71]. In particular, quadrature amplitude modulation (QAM) is one of the most spectrally efficient modulation formats [72]. This technique is also important with a view to enhancing the tolerance to dispersion and polarisation-mode dispersion (PMD) as well as to reduce the power consumption, as it enables us to realise a high-speed system with low speed devices.

In the first part of this section, we describe ultrahigh-speed OTDM transmission using the time-domain optical Fourier transformation (OFT) technique. By employing OFT, 640 Gbit/s/channel single-polarisation DPSK transmission over 525 km was successfully demonstrated. In the latter part of this section, we describe a 256 QAM coherent optical transmission. 64 Gbit/s (polarisation-multiplexed 4 Gsymbol/s, 256 QAM) data were successfully transmitted over 160 km with a 5.4 GHz optical bandwidth, which corresponds to a spectral efficiency of more than 11 bit/s/Hz in a single channel.

5.2. Ultrahigh-speed OTDM transmission

Single-channel transmission beyond 1 Tbit/s is expected to be the technological driving force for constructing next-generation ultrahigh-capacity optical transport networks such as terabit Ethernet. The first Tbit/s/ch transmission experiment was reported in 2000, in which a 1.28 Tbit/s polarisation-multiplexed OOK signal (640 Gbaud) was transmitted over 70 km [73]. Since then, attempts have been made to extend the transmission distance by adopting advanced modulation formats such as DPSK and DQPSK as shown in Fig. 19. By adopting DQPSK, polarisation-multiplexed 2.56 Tbit/s-160 km transmission has been demonstrated [74]. In these experiments, the symbol rate is 640 Gbaud. Since the pulse interval in a 640 Gbaud transmission is only 1.5 ps, such a high-speed transmission requires sub-picosecond pulses and therefore the system performance becomes vulnerable not only to chromatic dispersion (CD) and PMD but also to higher-order CD and PMD. This has limited the maximum transmission distance to 100–200 km.

Recently, we proposed a time-domain OFT technique [75] to cope with such transmission impairments. Time-domain OFT, in which the spectral profile is converted into a waveform in the time domain, makes it possible to eliminate the signal distortions that result from linear transmission impairments in optical fibres, such as jitter, dispersion slope, higher-order PMD, and time-varying perturbations. Here we present a single-polarisation 640 Gbit/s DPSK transmission over 525 km using the time-domain OFT technique, which is the longest transmission distance at a symbol rate of 640 Gbaud yet reported [76]. The OFT technique is successfully applied to a 640 Gbit/s DPSK signal, in which the strong chirp required for the OFT of a sub-picosecond pulse is realised with a phase modulator operated in a round-trip configuration.

The experimental setup for a 640 Gbit/s-525 km DPSK transmission is shown in Fig. 20. As an optical pulse source, we used a 40 GHz mode-locked fibre laser (MLFL) that generates a 2.0 ps pulse train at 1540 nm via mode-hop-free operation with an etalon installed in the cavity. To obtain the sub-picosecond pulse train required for 640 Gbit/s, we employed external pulse compression based on spectral broadening using self-phase modulation (SPM) in a fibre with

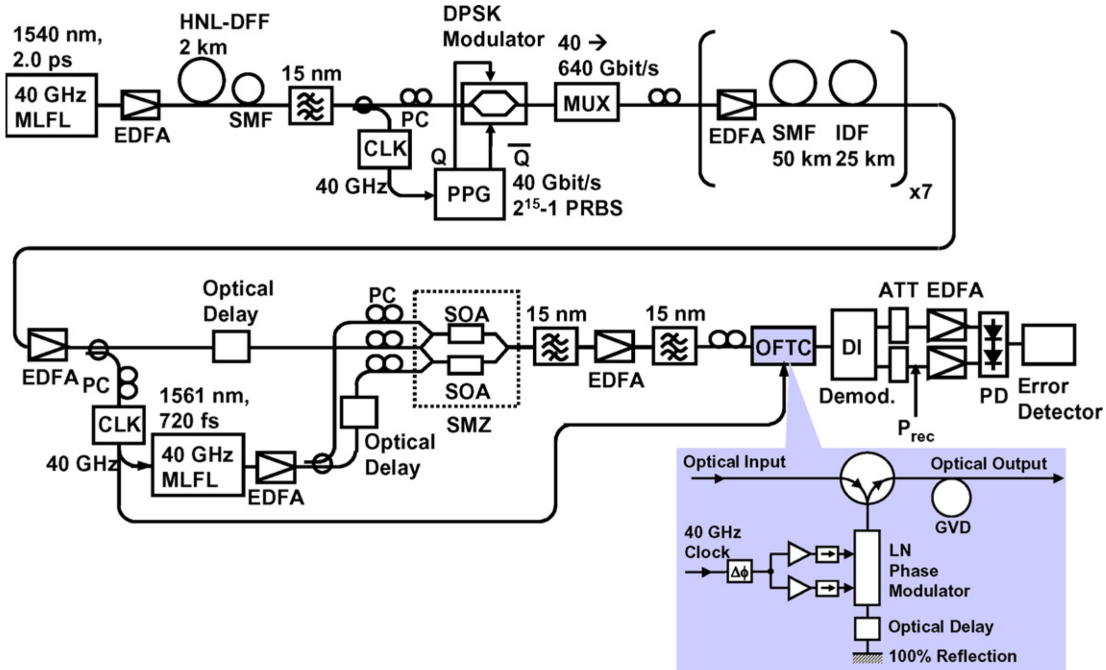

Fig. 20. Experimental setup for a 640 Gbit/s-525 km DPSK transmission.

normal dispersion. The MLFL output pulse was amplified to 20.5 dBm and launched into a 2 km highly-nonlinear dispersion-flattened fibre (HNL-DFF) with a dispersion of -0.2 ps/nm/km, a dispersion slope of 0.002 ps/nm^2/km and a nonlinear coefficient $\gamma = 5\ \mathrm{W}^{-1}\,\mathrm{km}^{-1}$. After chirp compensation with a single-mode fibre (SMF), the pulse was compressed to 600 fs.

The compressed pulse was DPSK modulated with a 40 Gbit/s, $2^{15} - 1$ PRBS, where the pulse pattern generator (PPG) was synchronised to a 40 GHz clock that was extracted after the pulse compression. The DPSK signal was then optically multiplexed to 640 Gbit/s with a single polarisation using an optical delay-line multiplexer, and launched into a 525 km transmission fibre. The fibre link consisted of seven 75 km spans of dispersion-managed fibre composed of standard single-mode fibre (SMF) and inverse dispersion fibre (IDF), which compensate for the dispersion and dispersion slope simultaneously. The total dispersion and dispersion slope were precisely compensated with a short piece of SMF at the end of the transmission link. The average DGD was 1.2 ps, which is almost the same as the bit interval. To mitigate the first-order PMD, the polarisation state of the 640 Gbit/s input signal was optimised to match the principal state of polarisation (PSP) of the 525 km fibre link with a polarisation controller (PC). The fibre loss was compensated at each span by using an EDFA. An optimal average input power to each span of +12 dBm was chosen to minimise OSNR degradation and nonlinear impairments. The pulse width after transmission estimated from an autocorrelation measurement varied between 630 and 730 fs when measured over a long period. The pulse broadening and its long-term variation are due to time-dependent second-order PMD, which induces time-varying polarisation-dependent CD.

On the receiver side, the 640 Gbit/s OTDM signal was demultiplexed to 40 Gbit/s with an all-optical semiconductor symmetric Mach–Zehnder (SMZ) switch [77], in which a 40 GHz MLFL emitting a 720 fs pulse operated by FM mode-locking was used as a control pulse source. The control pulse wavelength was set at 1561 nm. The MLFL was PLL-operated with a 40 GHz clock extracted from the 640 Gbit/s data using an electro-optical PLL clock recovery unit [78]. The optical power of the data and control pulse were set at 15 and 12 dBm, respectively. The polarisation state was adjusted with an automatic PC. At the SMZ output, the demultiplexed signal was separated from the control pulse with 15 nm optical filters, in which the pulse width was broadened to 1.1 ps.

The demultiplexed DPSK signal was then launched into an optical Fourier transform circuit (OFTC). OFT can be realised with linear chirp with a chirp rate K followed by a dispersion medium where $D = \beta_2 L$ that satisfies $K = 1/D$. To realise the strong chirp required for OFT for a sub-picosecond pulse, we adopted a phase modulator operated with a round-trip configuration. The optical pulse is first launched into the modulator in the forward direction, and phase-modulated by the RF signal travelling in the same direction. The optical pulse is then reflected and launched into the modulator in the backward direction, where the pulse is phase-modulated by the backward-travelling RF signal. This allows us to obtain a chirp twice as large as that obtained in an unidirectional phase modulator. We obtained a modulation depth of $M = 3.6\pi$, corresponding to a chirp rate $K = M\omega_{\mathrm{m}}^2 = 0.71\ \mathrm{ps}^{-2}$ at $\omega_{\mathrm{m}} = 2\pi \times 40$ GHz. The demultiplexed 40 Gbit/s DPSK signal was finally converted to an OOK signal with a one-bit delay interferometer (DI), and the bit error rate (BER) was measured after detection with a balanced photo-detector (PD).

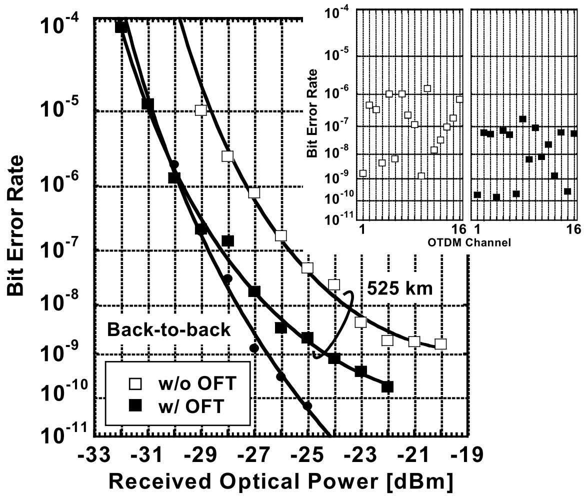

Fig. 21. BER characteristics for 640 Gbit/s-525 km transmission.

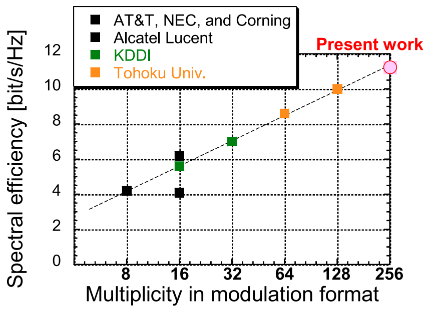

Fig. 22. Recent transmission experiments with high spectral efficiency.

The BER characteristics of the 640 Gbit/s-525 km transmission for the best OTDM channel are shown in Fig. 21. When OFT was not employed there was an error floor in the BER performance, and the best BER was of the order of 10^{-8} to 10^{-9} and varied with time, as a result of the time-dependent higher-order PMD. On the other hand, when OFT was employed, error-free performance with a BER of below 10^{-9} was achieved with a power penalty of only 2 dB. The insert in Fig. 21 shows the BER for all the OTDM tributaries measured with a received power of −16 dBm. The performance variation among different tributaries is attributed to intersymbol interference induced at the overlapping tails between adjacent pulses. A BER improvement of more than one digit was realised with OFT, and the stability against time-varying perturbations such as PMD and coherent crosstalk between adjacent pulses was also improved. The obtained BER performance was sufficiently below the standard FEC threshold (2×10^{-3}) for error-free operation.

5.3. Ultra-multilevel QAM coherent transmission

Coherent quadrature amplitude modulation (QAM) has attracted much attention with a view to increasing the spectral efficiency toward the Shannon limit. QAM is a modulation format that combines two carriers whose amplitudes are modulated independently with the same optical frequency and whose phases are 90 degrees apart. These carriers are called in-phase carriers (I) and quadrature-phase carriers (Q). 2^N QAM signal processes N bits in a single channel, so it has N times spectral efficiency compared with OOK (On-off-keying). The ultimate spectral efficiency is given by the Shannon limit[2]:

$$\frac{C}{W} = \log_2\left(1 + \frac{E_b}{N_0}\frac{C}{W}\right),$$

which is known as the Shannon–Hartley theorem [79]. The spectral efficiency of M-QAM approaches closer to the Shannon limit than other advanced modulation formats such as PSK or FSK, as the QAM multiplicity M increases.

Recent transmission experiments with high spectral efficiency are shown in Fig. 22. A 10 × 112 Gbit/s polarisation-multiplexed (Pol-Mux) 16 QAM transmission was demonstrated with a spectral efficiency of 6.2 bit/s/Hz [80], and an

[2] C [bit/s] is the channel capacity, W [Hz] is the bandwidth, E_b [J] and N_0 [W/Hz] are the bit energy and noise, respectively.

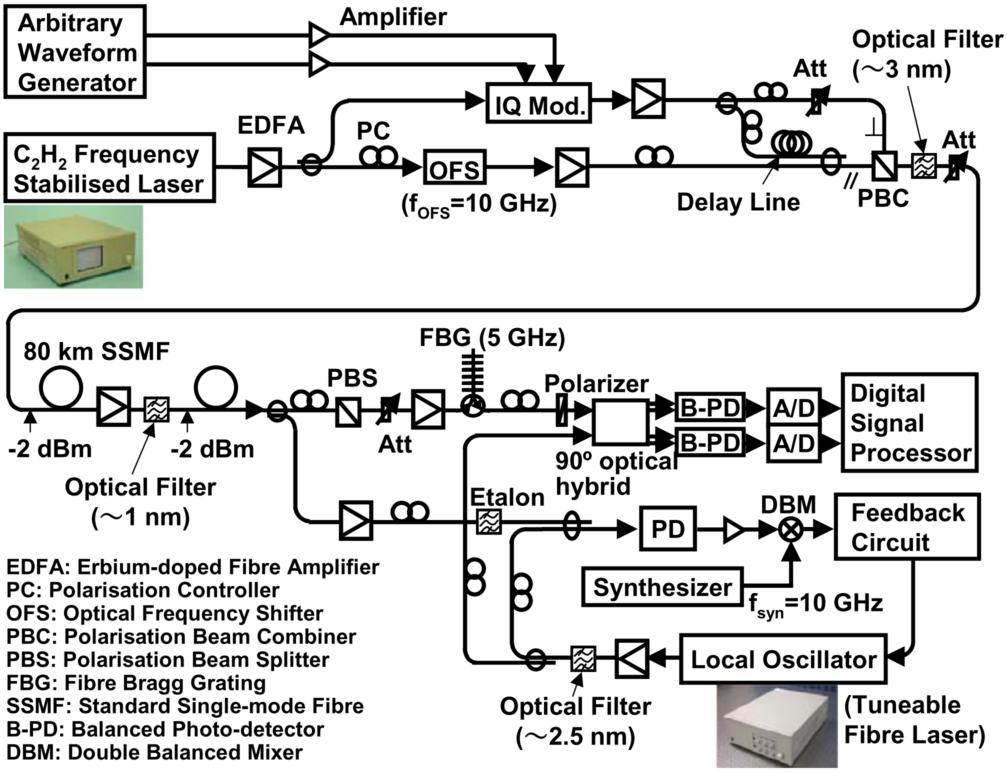

Fig. 23. Experimental setup for 4 Gsymbol/s, 256 QAM transmission.

8×65.1 Gbit/s Pol-Mux, orthogonal frequency division multiplexing (OFDM) transmission with a spectral efficiency of 7.0 bit/s/Hz was realised by using a sub-carrier modulation with 32 QAM [81]. To increase the spectral efficiency further, it is important to increase the multiplicity of the modulation level with sufficient SNR and IF frequency stability. Here we describe a 256 QAM coherent optical transmission with a Pol-Mux, 4 Gsymbol/s scheme over a 160 km standard single-mode fibre (SSMF) [82]. In this scheme, 64 Gbit/s data were transmitted with an optical bandwidth of 5.4 GHz.

The transmission setup is shown in Fig. 23. As a coherent light source, we employed a C_2H_2 frequency-stabilised fibre laser [83], whose linewidth is 4 kHz and the frequency stability is 1.3×10^{-11}. The coherent light is QAM modulated with an IQ modulator, where the beam is modulated with a 4 Gsymbol/s, 256 QAM baseband signal generated by an arbitrary waveform generator (AWG) running at 8 Gsample/s. We adopt a Nyquist filter with a roll-off factor of 0.35 at the AWG using a piece of software [84] that enables us to reduce the bandwidth of the QAM signal to 5.4 GHz. After the modulation, the QAM signal is coupled with a pilot tone signal whose frequency is 10 GHz down-shifted against the data signal.

After the transmission, the QAM signal is homodyne-detected with a local oscillator (LO) to convert the QAM data into a baseband signal. Here we employed an optical phase-locked loop (OPLL) technique to lock the optical phase between LO and QAM signal using the transmitted pilot tone, in which a high-speed free-running fibre laser is used as an LO. In the coherent receiver, the LO output is divided with a 90-deg phase shift each other and coupled with the QAM signal in a 90-deg optical hybrid circuit so that the cosine (I) and sine (Q) components are obtained after balanced detection. The phase noise of the detected signal was as low as 0.3 deg, which is sufficiently small for demodulating a 256 QAM signal. Finally they are A/D converted and demodulated into a binary sequence in the DSP. Because of the software demodulation, this transmission system operates in an off-line condition.

The BER performance for the Pol-Mux, 4 Gsymbol/s, 256 QAM transmission is shown in Fig. 24. Here, the maximum data length for demodulation was limited to 4096 symbols owing to the DSP memory size, which corresponds to a BER limit of up to 3.1×10^{-5}. In the back-to-back result, the received optical power at BER $= 2 \times 10^{-3}$ was $P_{\mathrm{rec}} = -32.0$ dBm, which corresponds to OSNR $= P_{\mathrm{rec}}/n_{\mathrm{sp}}h\nu\Delta\nu = 28.6$ dB and $E_{\mathrm{b}}/N_0 = \mathrm{OSNR}(\Delta\nu/R) = 20.9$ dB, where $\Delta\nu$ is the detection bandwidth of the optical signal and R is the data rate per polarisation. This value is close to the theoretical limit of $E_{\mathrm{b}}/N_0 = 18.7$ dB for 256 QAM [85]. This 2.2 dB difference may be attributed to the imperfect implementation of such hardware as the AWG and the IQ modulator.

The power penalty at a BER of 1×10^{-3} was approximately 5.3 dB for both polarisations, but both sets of polarisation data achieved a BER lower than the FEC limit of 2×10^{-3}. Figs. 24(b) and 24(c) show constellation maps for the back-to-back condition and after a 160 km transmission, respectively, at a received power of -21 dBm. Almost the same constellation was obtained for parallel polarisation. As a result, 64 Gbit/s data were transmitted over 160 km under the FEC threshold with an optical bandwidth of 5.4 GHz, which indicates the possibility of realising a spectral efficiency as high as 11.8 bit/s/Hz

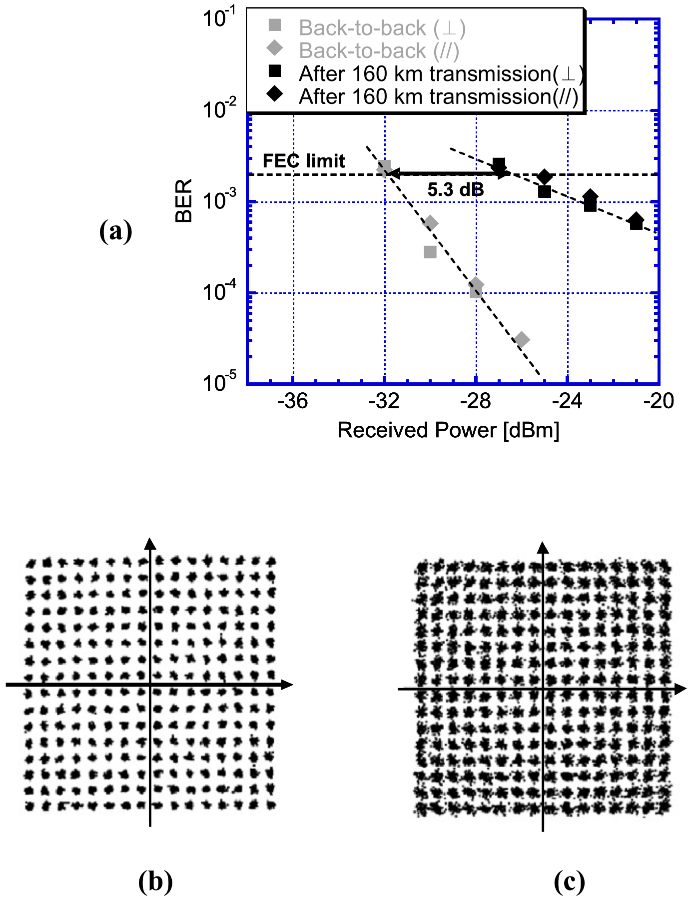

Fig. 24. Experimental results of 4 Gsymbol/s, 256 QAM transmission over 160 km. (a) BER characteristics, (b) and (c) constellations (4096 × 4 symbols) before and after 160 km transmission, respectively.

in a multi-channel transmission even when taking account of the 7% FEC overhead. An error-free transmission with a QAM as high as 256 levels requires an increase in the SNR at the transmitter and the receiver, a narrow band optical filter to remove amplified spontaneous emission (ASE) noise, and a large core fibre to reduce the fibre nonlinearity.

5.4. Conclusions

Two emerging optical transmission technologies, i.e. ultrahigh-speed OTDM transmission and coherent QAM transmission, were described. As regards the ultrahigh-speed transmission, we have adopted a time-domain OFT technique for improving the tolerance to higher-order PMD and demonstrated 640 Gbit/s/channel-525 km DPSK transmission. By combining this approach with polarisation multiplexing and DQPSK modulation, we can expect to achieve a long-haul transmission as fast as 2.56 Tbit/s/channel. As regards the coherent transmission, 256 QAM transmission was realised with a frequency-stabilised fibre laser and an optical PLL technique, which indicates the possibility of spectral efficiency as high as 11 bit/s/Hz. These technologies play important roles for realising advanced high-speed optical backbone networks and ultra-efficient, large capacity access networks.

6. Fibre technology for next generation networks

6.1. Introduction

Driven by society's ever increasing data capacity demands, it is clear that the next generation of telecommunication networks will be radically different from previous implementations; as we have seen in previous sections, multilevel coherent transmission and powerful digital signal processing will be deployed to maximise cable capacity. However, whilst these developments are welcome, they will only delay an inevitable "capacity crunch" as we exhaust the capacity of conventional single mode fibre. Put simply, once these techniques are deployed over the coming years and the capacity of current transmission line technology is reached we will only be able to increase network capacity by lighting additional fibres – a far from attractive solution from an economic perspective. With a Compound Annual Growth Rate (CAGR) of over 40% [86], this only delays a total capacity exhaust by a few years before new cable deployments are required (presumably at 40% of the installed base per annum using current fibres). However, the proximity of extensive deployment of new cables in the next decade (2020–2030) provides a unique opportunity to re-examine our choice of transmission fibre in the hope of finding a dramatic increase in per-fibre capacity. It is therefore clear that radical innovation in the basic internet infrastructure (i.e. transmission fibres and amplifiers) is now urgently required. Moreover, the technology will need to be commercialised rapidly if we are to avoid this potential capacity crunch.

Unsurprisingly perhaps, many of the key issues to be faced in developing the next generation of fibres for telecommunication (e.g. nonlinearity, mode-control, and damage effects) are also critical in the context of high power fibre lasers. Consequently, we anticipate that much of the work done in this field, which has led to power scaling of fibre lasers from the 100 W to the 10 kW regime over the past decade, may be leveraged to good effect as we look to further capacity scale our networks.

6.2. Enhancing the fibre capacity

In order to increase the capacity of a single optical fibre cable one can pursue a number of options either separately or preferably in combination:

(1) *Reduce the loss and nonlinearity of the transmission line*. In order to maximise the data carrying capacity of a fibre it is necessary to operate with as high a signal spectral efficiency (and corresponding OSNR) as possible before the onset of the nonlinear impairments that ultimately compromise performance [87]. The reduction of nonlinearity and attenuation are thus primary targets for next generation transmission fibres. The incorporation of some form of signal regeneration can also be gainfully employed to help reduce the impact of nonlinearity and provide access to higher spectral efficiencies [88].

(2) *Increase the number of separate information channels carried within the fibre* using some form of spatial division multiplexing to increase the data capacity per unit cross sectional area of the fibre. Different forms of spatial division multiplexing can be adopted, either within the same core (multi-mode transmission) or within the same fibre (multi-core transmission).

(3) *Extend the usable spectral bandwidth* beyond the C + L band as currently used – this requires the development both of a transmission fibre with a suitably low-loss transmission window and an associated low-noise optical amplifier technology.

Clearly, in applying any new technique it is necessary to be mindful from the outset both of the optical power handling and mechanical properties of the fibres and the associated overall electrical power requirements. In the following sections various technical options to realise the above targets are reviewed.

6.3. Transmission fibres with reduced loss and nonlinearity

6.3.1. Lower-loss silica fibres

To date, the lowest loss reported for a silica fibre, obtained with a pure silica core, is 0.148 dB/km [89]. This is very close to the theoretical minimum for such a glass, meaning that there is very little scope for further improvement. The minimum loss is determined by the levels of Rayleigh scattering and the proximity of the infrared absorption edge within the core glass. The level of Rayleigh scattering can be reduced by lowering the fictive temperature of the core glass – which is extremely high in silica – hence the 2000 °C processing temperature [90]. One possible way to reduce the Rayleigh scattering is therefore to lower the melting temperature of the glass, which can be done by suitable doping of silica. For example, in [91], it was predicted that a 20–30% loss reduction down to the 0.11 dB/km level should be achievable using a P_2O_5-F-silica based core. Practical realisation of such a fibre will require chemical vapour deposition (CVD) techniques to ensure ultra-high purity and the search for a thermally compatible cladding material with acceptable loss and environmental stability.

6.3.2. Non-silica fibres

Owing to its excellent material processing characteristics and low optical loss, silica is an almost ideal fibre material. However, there are a range of materials, most notably fluoride glasses, which potentially offer substantially lower intrinsic losses than silica [92]. Indeed, the theoretical minimum loss of several fluoride glasses is predicted to be as low as 0.03 dB/km at wavelengths around 2.5 μm. Significant research programs ran around the world until the early 1990s that attempted to draw fibres with a lower loss than silica and significant progress was made with losses as low as 0.65 dB/km reported by researchers at BT Research Laboratories [93]. With the development of the erbium doped fibre Amplifier (EDFA) and the difficulty of working with fluoride glasses (which are both hygroscopic and tend to produce fragile fibre) this work was stopped in the early 1990s. However, with a looming capacity crunch and with the significant advances made in material purification and gas phase deposition in the past 20 years, it may be time to revisit this topic and to undertake fundamental materials/glass studies and fibre drawing trials to re-assess the prospects of this approach.

6.3.3. Photonic bandgap fibres

Hollow-core Photonic Band Gap Fibres (PBGFs) represent a technology that could potentially yield major benefits in terms of both loss and nonlinearity. PBGFs comprise an array of longitudinal wavelength-sized holes periodically arranged in the cladding to form a photonic bandgap in the transverse plane of the fibre, and an air-filled hollow core in which light is constrained to propagate over a tailorable spectral range [94]. The sub-percent fraction of optical power guided in the glass

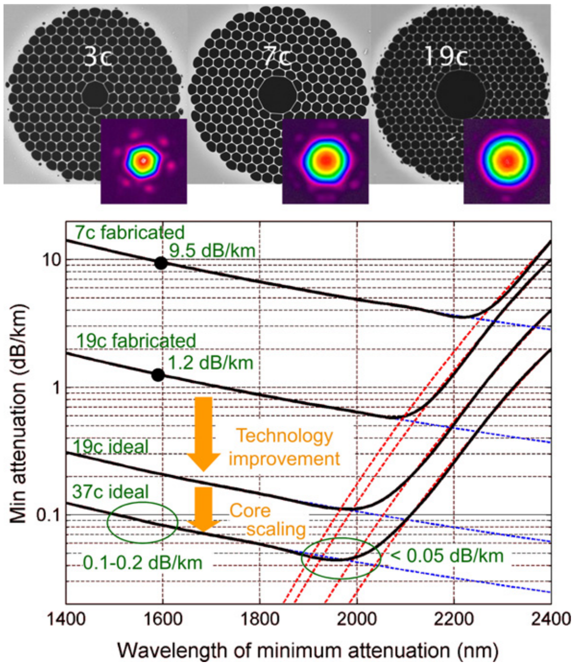

Fig. 25. Top – various SEM images of PBGFs with different core sizes and associated fundamental mode images. Bottom – fundamental mode loss versus wavelength for different core designs showing the expected loss improvements due to better technological approaches to fibre manufacture and further scaling of the core size.

matrix means that Rayleigh scattering, the dominant source of loss for conventional solid core fibres, is negligible for PBGFs, such that these fibres have the potential to achieve significantly lower losses than conventional solid core variants [95].

Losses in PBGFs are fundamentally dominated by two mechanisms: (1) surface scattering at the core glass–air interface; and (2) infrared phononic absorptions in the glass matrix. The former has a λ^{-3} wavelength dependence as opposed to the conventional λ^{-4} due to Rayleigh scatting in solid core glass fibres, while the latter is significantly reduced as compared to conventional fibres due to the much smaller percentage of power guided in the glass. The combined effect of these two loss mechanisms is to shift the wavelength region of minimum loss from 1550 nm to the 1900–2100 nm band [95,96]. Impressive improvements in PBGF design and fabrication techniques have reduced the loss in these fibres from several dB/m to 1.2 dB/km at 1600 nm in the space of just a few years (see Fig. 25). The potential for nonlinearity reduction relative to solid core fibres is, however, even more significant due to the very low nonlinearity of air and the low mode overlap with silica [97]. Indeed, fibres with around 1/1000th of the nonlinearity of conventional solid fibres have already been achieved and have been exploited for beam delivery in fibre laser systems, particularly in short pulse systems where peak powers in excess of 1 MW have been reported. Such a small nonlinearity can be exploited to increased signal power levels and to reduce nonlinearly induced cross-talk.

Our modelling indicates that through realistic technological improvements in fibre fabrication and optimised fibre designs it might be possible to realise fundamental mode losses below 0.1 dB/km, representing up to 20 times improvement over the current 1.2 dB/km record (achieved in a fibre with a large core obtained by merging together 19 cladding holes [95]), see Fig. 25. This would allow for both reduced noise or increased amplifier spans depending on system design. Our estimate is based on a 4-fold expected reduction in surface scattering due to improvements in surface roughness ($\times 2$) and to the use of longer transmission wavelengths ($\times 2$), and a further five-fold combined improvement resulting from a reduced electromagnetic field intensity at the glass surface arising from use of a larger core ($\times 2.5$) and a higher air fill fraction cladding ($\times 2$). These fibres would have a nonlinear coefficient extremely close to that of air ($\gamma \sim 0.001\ \mathrm{W}^{-1}\ \mathrm{km}^{-1}$) and a low-loss bandwidth potentially exceeding the bandwidth of current S + C + L band systems, assuming issues associated with residual gas and water species absorptions can be dealt with. Note that in order to be able to fully exploit these fibres it will also be necessary to deal with the increased number of modes that will be supported by the larger core, as well as the practical issues of long-term reliability, interconnection and cabling.

6.4. Fibres for spatial division multiplexing

From an information theory viewpoint, a multi-mode fibre has a far larger information transport capacity than a single-mode fibre. It guides a multitude of modes, each of which can in principle have a capacity equal to the capacity of a conventional fibre. However, the use of individual modes within large core to provide multiple channels clearly represents a significant challenge, with crosstalk (mode-mixing) likely to prove a major hurdle that will rapidly limit performance. One

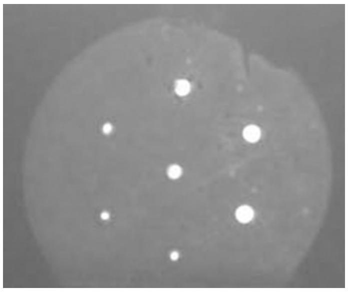

Fig. 26. A 7-core fibre with dissimilar cores fabricated at the ORC. Note that this particular fibre is an active fibre design for high power laser applications.

potential away to mitigate the effects of cross-talk is to adapt and apply the concept of Multi-Input Multiple Output (MIMO) technology successfully used to reduce the impact of multipath interference in radio communications to the optical domain [98,99].

An alternative and potentially much simpler approach is to use a single fibre structure encompassing a number of independent single-mode fibre cores. In the simplest incarnation, each identical core is independent of all other cores and the cores are kept well isolated from each other. This requires careful design of the core and core-spacing in order to reduce mode coupling whilst at the same time ensuring low propagation and bending losses. One option to increase the packing density is to ensure that the individual neighboring cores are different and thus have different propagation constants so that mode-coupling is reduced [100]. (See Fig. 26 for such a fibre produced for high power laser applications.) Initial estimates are that 7-cores might be accommodated in a 125 μm fibre by appropriate design, and 19 in a 160 μm structure with significant scope for further optimization remaining.

Note that since first writing this article interest in spatial division multiplexing (both multimode and multi-core) has increased substantially and very rapid progress has been made – to the extent that 6 out of 34 papers in the Postdeadline session at the very recent Optical Fibre Communications Conference 2011 (OFC 2011) were on this topic alone. We refer the reader to the proceedings of this conference for a detailed view of the current state-of-the-art [101].

6.5. Fibres with improved power handling

An increased fibre capacity will obviously lead to higher average power levels within the fibre, with the consequence that we will rapidly encroach upon the ∼1.2 W fibre fuse threshold for SMF [102]. Any new fibre technology will therefore need to be developed with this in mind. Power handling is fundamental to the realisation of robust, reliable high power fibre laser systems and substantial progress has been made in the management of scattered/unconfined light and thermal effects in fibres. This knowledge, perhaps coupled with the observation that the fuse threshold can be increased though the use of microstructure within the fibre [103], should ensure that the need to use higher power levels will be a solvable problem from a cable reliability perspective. The issues of eye-safety and the associated increased electrical power requirements for optically amplified submarine systems may though prove thornier problems.

6.6. Next generation optical amplifiers

6.6.1. Rare earth-doped amplifiers above the L-band

For both low-nonlinearity PBGF fibres and fibres made from new low loss materials, such as fluoride glass, the minimum loss wavelength will extend towards and potentially beyond 2 μm. The development of amplifiers capable of operating in this spectral region is thus an important technical requirement. Rare earth (RE) doped fibres based on either thulium or holmium appear to be the most attractive solutions, as they are diode-pumpable and operate in the spectral regime from 1.7–2.2 μm [104,105]. Tm^{3+}-doped silica fibre lasers and amplifiers have received increasing attention over the past few years as a result of emerging applications in the medical, defence and security areas. So far the work has focused on realising high power, single wavelength lasers and output powers approaching 1 kW have already been reported [106]. The use of these RE/silica systems as amplifiers has only started relatively recently and so far not with optical fibre telecommunications in mind.

To ensure low noise it is highly desirable to use a core pumping scheme. Exploiting the well-known 2-for-1 cross relaxation process that takes place in Tm when pumping at 0.8 μm increases efficiency and avoids the heat load associated with the large quantum defect. For this, a high doping concentration is essential and this leads to a very short device length that could be attractive for integrated planar devices. Alternatively, a longer pump wavelength of 1.6 μm might be employed. This choice offers the additional benefits of avoiding any up-conversion processes and their possible effect on photo-darkening. In order to extend operation still further to the 2.5–2.8 μm region, where the minimum loss for many potential low intrinsic loss soft glass compositions lie, a change of glass host from silica to a lower phonon energy host glass will be required. Candidate materials include both tellurite and fluoride glasses.

6.6.2. Rare earth-doped amplifiers below the C-band

The development of low water loss fibres such as OFS “All-Wave” means that fibre amplifiers are now needed for the 1.3–1.5 μm range, extending perhaps to even shorter wavelengths for distribution/datacomms applications. Candidate options include Raman amplifiers [107], RE ions in low phonon energy materials such as ZBLAN and tellurite glasses [105], neodymium-doped fibres [105] and, most recently, bismuth-doped fibres [108]. Gain from bismuth-doping came as a surprise to the community and the underlying mechanisms by which the gain is obtained are still not well understood, highlighting the continued importance of fundamental material studies. Powerful emerging in-fibre distributed filtering technologies based on antiresonant effects such as those exploited in all-solid bandgap fibres [109] will also be helpful to suppress unwanted transitions.

An alternative approach to RE-fibre amplification with its defined windows of operation is Raman scattering, which can provide gain at any wavelength within the transparency window of the host glass [107]. Moreover, by shaping the pump spectrum one can control the gain spectrum to ensure flat gain. While an established technology, application has been restricted primarily to distributed amplification in long haul systems to complement the use of the EDFA, rather than as a discrete amplifier. Traditionally, Raman amplifiers are pumped using arrays of semiconductor lasers, or by Raman lasers based on complex cascaded resonators formed of nested gratings, or arrays of couplers. Whilst such amplifiers can give reasonable performance it is difficult to get truly broadband coverage in a compact device. Developments in fibre laser technology open up new pumping options. For example, the use of counter-propagating, rectangular-shaped optical pulses of differing amplitudes to synthesise complex, broadband gain spectra for pumping lumped Raman amplifier configurations [110].

6.6.3. Amplifiers for spatial division multiplexed systems

With significant interest growing in SDM the need for amplifiers compatible with SDM transmission fibres emerges. From a cost and simplicity perspective such an amplifier would ideally amplify all spatial channels simultaneously (be they individual modes or separate cores). Given the noise and cross-talk requirements this represents a huge challenge and to date little (if any) progress has been reported. The option of demultiplexing the individual channels and the use of multiple conventional (single-mode) amplifiers (one per spatial channel) followed by a further multiplexing process always exists and perhaps provides a more realistic, albeit less attractive, approach – although, even here, many challenges exist at the component level. Without a practical, cost-effective amplifier solution the use of SDM for long haul transmission is clearly likely to be of very limited interest.

6.6.4. Phase sensitive parametric amplifiers

All-optical communication systems use optical amplifiers to compensate for fibre loss. Current systems based on conventional binary modulation formats, e.g., NRZ or RZ, use either erbium-doped or Raman fibre amplifiers, both of which produce signal gain that is independent of the phase of the signal, and are thus classified as Phase Insensitive Amplifiers (PIAs). Such amplifiers are extremely robust and offer exceptional multi-wavelength system capabilities, but add quantum noise to the signal that compromises performance. A second (parametric) form of amplification based on nonlinear optics offers Phase Sensitive Amplification (PSA). PSA can give low-noise operation (theoretically noise-free for certain implementations) [111,112], phase-regeneration [113], and interesting photon correlation characteristics that are important to quantum information transmission and processing [114]. With the emergence of higher order Phase Shift Keying (PSK) signals that rely upon phase coding, the question naturally emerges as to whether the use of PSA offers new opportunities in future optical networks. In recent works both $\sim$ 1 dB NF amplification [115], and high quality regeneration of binary PSK signals at data rates as high as 40 GBit/s [116] have been demonstrated using an in-line “black box” implementation, which represents a significant step forward in terms of practicality.

In Fig. 27 we show typical input and output constellation and eye diagrams measured on 10 Gbit/s DPSK data in the absence (left) and presence (right) of a significant sinusoidal phase perturbation ($\pm$70 degrees sinusoidal modulation at 5 GHz). The measurements illustrate the drastic phase noise reductions that can be achieved due to the periodic 2-level phase response of the PSA.

The implications of a practical PSA technology within optical communications could potentially be profound, offering benefits such as: improved OSNRs – providing increased flexibility in terms of the constellation diagrams that might be used for M-PSK signals; reduced signal power requirements and associated nonlinear effects and; novel optical processing elements for M-PSK signals, including single and multichannel all-optical regenerators and monitoring devices.

6.7. Conclusions

In conclusion, we have described some of the major challenges facing network operators and designers trying to provision for the continued growth in internet traffic. It is clear that innovation in the underlying fibre infrastructure will be required soon to avoid the looming capacity crunch that is likely to hit us within the next 10–15 years.

We have discussed a number of opportunities that if employed in isolation could provide around one order of magnitude improvement in transmission capacity for a single fibre and in combination perhaps up to two orders of magnitude improvement, enabling Petabit/s transmission. Clearly to realise this in practise will represent an enormous engineering challenge; however it is one that needs to be addressed in order to service societies increasing digital needs and expectations.

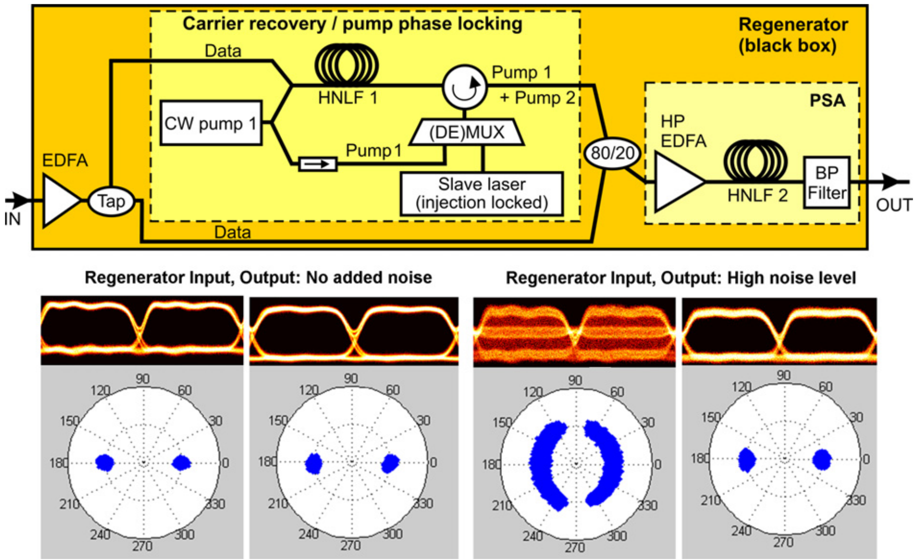

Fig. 27. Top – PSA implementation. Bottom – constellation and eye diagrams at PSA input (LHS) and output (RHS). Almost perfect signal quality is restored when substantial phase noise is added to the input signal S [29].

7. Conclusion and perspectives

The field of optical communications traces back from the invention of the laser (1960) and relatively soon after, the optical fibre (1966 to 1970); in turn, it is approaching its own "half-century maturity". Since the original lab and industry vision, and beyond reasonable prediction, so much inventive technology has been accomplished indeed, in order to reach the current state of art! While the same observation applies to radio cellular and satellite communications, optical technologies made the global network backbone, the high-speed Internet, a reality.

As we described it in Section 1, the originating optical communications breakthrough was the transition, from optical fibres with 1 dB/m attenuation, to low-loss optical fibres, nowadays manufactured with 20 dB/100 km loss. Such transparent "lightpipes", keep laser-light coherence and signal integrity over distances of one-hundred kilometres/miles. Over the same early period, semiconductor technology ensured the development of narrow-spectrum, microchip-scale, highly-reliable and efficient laser sources and photo-detectors. Altogether, optical communications technology would bring *bandwidth*.

The electronic bottleneck of early "repeaters", which, in the early 1980s circumscribed the geographical horizon of optical telecoms, was alleviated through yet another sweeping revolution: in-line amplification by stimulated emission through *erbium-doped fibres*, the EDFA. Several wavelength channels could then be periodically repowered "at once", without mutual interference. Hence the golden age of WDM, which, in its early stage, one may rightly call the era of "virtually unlimited bandwidth". Alternatively, it could be called as well the era of "conquest for bandwidth", because highly sophisticated means to appropriate such a potential had to be invented and deployed. Thus, the world currently enjoys "global bandwidth", which is as much a hardware as a software concept, the first being generally overlooked from any end-user standpoint.

Then, what about the remaining challenges lying ahead in our "modern telecommunications"?

Next, we have seen (Section 2) that discrete transmit/receive components, mostly InP-based, are at the root of the optical communication industry. Yet, improving their characteristics towards higher performance in speed, chip size, electro-optical conversion efficiency and high temperature operation remains a major challenge for the coming decade. This technology will have to meet a growing transmission capacity demand, while offering the increased requested wavelength agility and, simultaneously, a low environmental cost, i.e. low energy/material consumptions. As for the societal impact, next to global connectivity, there are emerging markets such as security, medical imaging, pollution sensing, to quote a few.

Section 3 has also highlighted the fact and reality that after 50 years, the utility of the laser continues to thrive and prosper. In this respect, large-scale Photonic Integrated Circuits utilising arrays of semiconductor lasers and photo-receivers, are no exception. More and more technology integration is key to massive or global deployment, at ever-reduced costs and energy savings.

But it is not all about components technology. Key concepts of high-bit-rate transmission had to be revisited, stretching system design to ultimate performance, exploring the boundaries of Physics and fundamental Laws. At the same time, the new solutions for "more transmission bandwidth" had to respect the basic engineering rules of simplicity, cost-effectiveness, and short time-to-market. Section 4 illustrated this through the revival of coherent detection. Along with digital signal processing, including powerful and efficient codes for error correction, and the introduction of multi-level modulation formats, a strong momentum has been gathered in high-speed, long-haul fibre links. Research is now all about breaking the current, status of 112 Petabit/s km performance.

The exploration of new frontiers in multi-level, ultrahigh-speed transmission has continued in Section 5, with focus on two emerging technologies, namely OTDM and coherent QAM transmission. In the first case, was shown that long-haul (> 500 km) transmission as fast as 2.56 *Tbit/s per channel* is achievable. In the second case, 256-level QAM transmission with the possibility of spectral efficiency as high as 11 bit/s/Hz, was described.

After optical components and system transmission come advanced fibre technologies, as described in Section 6. These promise new potentials in single-fibre transmission capacity, power-handling, and extended/broadband optical amplification, which are the three key factors to meet the upcoming bandwidth challenge. Namely, such a challenge in the next decade is the continued growth in internet traffic, which means the continued provisioning and quality of service, of the global network connectivity, altogether at ever-higher rates and affordable end-user costs.

Acknowledgements

D. Richardson et al. would like to thank their many colleagues for useful discussions and inputs in relation to the work and ideas presented in this paper – in particular to Dr. N.G.R. Broderick relating to band gap fibres, Drs. P. Petropoulos, F. Parmigiani, R. Slavik and Mr. J. Kakande in relation to PSAs and Prof. J. Nilsson, Prof. M.N. Zervas, Prof. W.A. Clarkson and Dr. J.K. Sahu for in relation to broadband amplifiers. In addition, D.J.R. would like to acknowledge many interesting and insightful discussions with Dr. A.D. Ellis of the Tyndall Institute Ireland, Prof. P. Andrekson of Chalmers University of Technology, Sweden and with Dr. T. Morioka of NTT Laboratories, Japan on concepts for next generation fibre technology. F.P. gratefully acknowledges the support of a Royal Society University Fellowship.

E. Desurvire is most grateful to this article's Guest Editor Prof. C. Labaune for entrusting the task of putting together this commemorative paper on Optical Communications, and to C. Kazmierski and D. Pons from Alcatel-Thales III-V Lab, to F. Kish and D. Welch from Infinera, to S. Bigo and J.-L. Beylat from Alcatel-Lucent, to Prof. M. Kakazawa from Tohoku University, to Prof. D. Richardson and Prof. D.N. Payne from the University of Southampton and all their co-author colleagues, for their enthusiastic, insightful and fruitful contributions to this common endeavour.

References

[1] K.C. Kao, G. Hockham, Dielectric fibre surface waveguide for optical frequencies, Proc. IEE 113 (7) (July 1966) 1151–1158.
[2] S.E. Miller, A.G. Chynoweth, Optical Fiber Telecommunications, Academic Press, San Diego, London, 1979, see also:
I. Kaminow, T. Li, Optical Fiber Telecommunications IV, Academic Press, San Diego, London, 2002.
[3] E. Desurvire, Erbium-Doped Fiber Amplifiers, Principles and Applications, J. Wiley & Sons, New York, 1994, and references therein; about EDFA theory and technologies, see also:
E. Desurvire, D. Bayart, B. Desthieux, S. Bigo, Erbium-Doped Fiber Amplifiers, Device and System Developments, J. Wiley & Sons, New York, 2004, and references therein.
[4] E. Desurvire, The golden age of optical amplifiers, Phys. Today 47 (1) (January 1994) 20; Japanese translation published in Parity 10 (3) (1995) 4–12.
[5] Jeff Hecht, The evolution of optical amplifiers, Optics & Photonics News (August 2002) 36.
[6] E. Desurvire, Capacity demands and technology challenges for lightwave systems in the next two decades, IEEE J. Lightwave Technology 24 (12) (2006).
[7] E. Desurvire, Classical and Quantum Information Theory, an Introduction for the Telecom Scientist, Cambridge University Press, 2009.
[8] E. Desurvire, Optical communications, C. R. Physique 4 (1) (2003).
[9] J.-C. Antona, S. Bigo, Recent advances in optical telecommunications, C. R. Physique 9 (9–10) (2008).
[10] Larry A. Coldren, Erik J. Skogen, James W. Raring, Jonathon S. Barton, Dan Lofgreen, Leif Johansson, Jonathan T. Getty, Active photonic integrated circuits (invited), in: IPRM 2005, 8–12 May, Glasgow, Scotland.
[11] E.J. Skogen, J.W. Raring, G.B. Morrison, C.S. Wang, V. Lal, M.L. Masanovic, L.A. Coldren, Monolithically integrated active components: a quantum-well intermixing approach, Selected Topics in J. Quantum Electron. 11 (2005) 343–355.
[12] C. Jany, J. Decobert, F. Alexandre, A. Garreau, J.-G. Provost, O. Drisse, E. Derouin, F. Blache, J. Landreau, N. Lagay, F. Martin, D. Carpentier, C. Kazmierski, 10 Gbit/s 1.55 μm 25 km transmission at 90 °C with new self thermally compensated AlGaInAs directly modulated laser, in: OFC/NFOEC, 27–29 March 2007, Anaheim CA (JWA32).
[13] Philippe Chanclou, Daniel Torrientes, Frank Chang, Benoit Charbonnier, Christophe Kazmierski, 10 Gbit/s for next generation PON with electronic equalization using un-cooled 1.55 μm directly modulated laser, in: ECOC 2009, 20–24 September, Vienna, Austria (PostDeadline3.5).
[14] C. Kazmierski, A. Konczykowska, F. Jorge, F. Blache, M. Riet, C. Jany, A. Scavennec, 100 Gb/s operation of an AlGaInAs semi-insulating buried hetero-junction EML, in: OFC 2009, 22–26 March 2009, San Diego CA (OThT7).
[15] R. Alferness, Plenary talk, in: ECOC2008, 21–25 September, Brussels, Belgium.
[16] Inuk Kang, S. Chandrasekhar, C. Kazmierski, M. Rasras, N. Dupuis, 1650-km transmission of 50-Gb/s NRZ and RZ-DQPSK signals generated using an electroabsorption modulators-silica planar lightwave circuit hybrid integrated device, in: OFC2010, 22–25 March, San Diego CA (OMJ4).
[17] D. Bimberg, M. Grundmann, N.N. Ledentsov, Quantum-Dot Heterostructures, John Wiley & Sons, 1999, and references therein.
[18] F. Lelarge, B. Dagens, J. Renaudier, R. Brenot, A. Accard, F. van Dijk, D. Make, O. Le Gouezigou, J.-G. Provost, F. Poingt, J. Landreau, O. Drisse, E. Derouin, B. Rousseau, F. Pommereau, G.-H. Duan, Recent advances on InAs/InP quantum dash based semiconductor lasers and optical amplifiers operating at 1.55 μm, J. Selected Topics Quant. Electron. 13 (1) (2007) 111–127 (invited paper).
[19] K. Merghem, A. Akrout, A. Martinez, G. Aubin, A. Ramdane, F. Lelarge, G.-H. Duan, Pulse generation at 346 GHz using a passively mode locked quantum-dash-based laser at 1.55 μm, Appl. Phys. Lett. 94 (2009) 021107.
[20] A. Akrout, A. Shen, R. Brenot, F. Van Dijk, O. Legouezigou, F. Pommereau, F. Lelarge, A. Ramdane, G.-H. Duan, Error-free transmission of 8 WDM channels at 10 Gbit/s using comb generation in a quantum dash based mode-locked laser, in: Proceedings of European Conference on Optical Communication (ECOC), Bruxelles, September 2008 (post-deadline paper).
[21] F. van Dijk, A. Enard, X. Buet, F. Lelarge, G.-H. Duan, Phase noise reduction of a quantum dash mode-locked laser in a millimeter-wave coupled opto-electronic oscillator, J. Lightwave Technol. 26 (15) (August 2008) 2789–2794.
[22] M. Huchard, P. Chanclou, B. Charbonnier, F. van Dijk, G.-H. Duan, C. Gonzalez, F. Lelarge, M. Thual, M. Weiß, A. Stöhr, 60 GHz radio signal up-conversion and transport using a directly modulated mode-locked laser, in: International Topical Meeting on Microwave Photonics Australia, October 2008 (post-deadline paper).

[23] J. Faist, F. Capasso, D. Sivco, C. Sirtori, A. Hutchinson, A. Cho, Science 264 (1994) 553.
[24] M. Carras, M. Garcia, X. Marcadet, O. Parillaud, A. De Rossi, S. Bansropun, Top grating index-coupled distributed feedback quantum cascade lasers, Appl. Phys. Lett. 93 (2008) 011109.
[25] A. Lyakh, R. Maulini, A. Tsekoun, R. Go, C. Pflügl, L. Diehl, Q.J. Wang, Federico Capasso, C. Kumar, N. Patel, 3 W continuous-wave room temperature single-facet emission from quantum cascade lasers based on nonresonant extraction design approach, Appl. Phys. Lett. 95 (2009) 141113.
[26] Richard Soref, Towards silicon-based longwave integrated optoelectronics (LIO), in: SPIE Photonics West, Silicon Photonics III, 21 January 2008 (invited paper 6898-5).
[27] R. Martini, E.A. Whittaker, Quantum cascade laser-based free space optical communications, J. Opt. Fiber. Commun. Rep. 2 (2005) 279–292.
[28] K. Kato, Ultrawide-band/high frequency photodetectors, IEEE Trans. Microwave Theory Tech. 47 (July 1999) 1265–1281.
[29] A. Umbach, D. Trommer, A. Sietke, G. Unterbörsch, Waveguide integrated photodetector with 45 GHz bandwidth, Electron. Lett. 32 (November 1996) 2143–2145.
[30] L. Giraudet, F. Banfi, S. Demiguel, G. Hervé-Gruyer, Optical design of evanescently coupled, waveguide-fed photodiodes for ultra-wide-band applications, IEEE Photon. Technol. Lett. 11 (January 1999) 111–113.
[31] A. Rouvié, D. Carpentier, N. Lagay, J. Décobert, F. Pommereau, M. Achouche, High gain-bandwidth product over 140-GHz planar junction AlInAs avalanche photodiodes, IEEE Photon. Technol. Lett. 20 (March 2008) 455–457.
[32] T.H. Maiman, Stimulated optical radiation in ruby, Nature 187 (6 August 1960) 493–494.
[33] R.N. Hall, et al., Coherent light emission from GaAs junctions, Phys. Rev. Lett. 9 (1 November 1962) 366–368.
[34] N. Holonyak Jr., S.F. Bevacqua, Coherent (visible) light emission from Ga(As1–x Px) junctions, Appl. Phys. Lett. 1 (December 1962) 82–83.
[35] M.I. Nathan, et al., Stimulated emission of radiation from GaAs p–n junctions, Appl. Phys. Lett. I (November 1962) 62–64.
[36] T.M. Quist, et al., Semiconductor maser of GaAs, Appl. Phys. Lett. 1 (December 1962) 91–92.
[37] Z.I. Alfërov, et al., Injection lasers based on heterojunctions in the AlAs–GaAs system with low threshold at room temperature, Fiz: Tekh. Polupr. 3 (September 1969) 1328–1332. Also Sov. Phys.-Semiconductor 3 (March 1970) 1107–1110.
[38] I. Hayashi, et al., Junction lasers which operate continuously at room temperature, Appl. Phys. Lett. 17 (1 August 1970) 109–111.
[39] E.A. Rezek, et al., LPE $In_{1-x}Ga_xP_{1-z}As_z$ ($x \sim 0.12$, $z \sim 0.26$) DH laser with multiple thin-layer (< 500 A) active region, Appl. Phys. Lett. 31 (15 August 1977) 288–290.
[40] D.R. Scifres, et al., Distributed feedback single heterojunction GaAs diode laser, Appl. Phys. Lett. 25 (15 August 1974) 203–206.
[41] K. Utaka, et al., Room-temperature CW operation of distributed-feedback buried-heterostructure InGaAsP/InP lasers emitting at 1.57 μm, Electron. Lett. 17 (25/26) (December 1981) 961–963.
[42] J.J. Hsieh, et al., Room-temperature CW operation of GaInAsP/InP double-heterostructure diode lasers emitting at 1.1 μm, Appl. Phys. Lett. 28 (1976) 709.
[43] S.E. Miller, Integrated optics: An introduction, Bell Sys. Tech. J. 48 (1969) 2059–2069.
[44] Y. Kawamura, et al., Monolithic integration of a DFB laser and an MQW optical modulator in the 1.5 μm wavelength range, IEEE JQE QE-23 (1987) 915–918.
[45] R. Nagarajan, et al., Large-scale photonic integrated circuits, IEEE JSTQE 11 (1) (January/February 2005) 50.
[46] S. Corzine, et al., Large-scale InP transmitter PICs for PM-DQPSK fiber transmission systems, IEEE Photonics Technology Letters 22 (14), 1015–1017, art. no. 5458061.
[47] G.E. Moore, Cramming more components onto integrated circuits, Electronics 38 (8) (19 April 1965).
[48] J.S. Kilby, Miniaturized electronic circuits, U.S. Patent 3,138,743, June 23, 1964 (filed 6 February 1959).
[49] R.N. Noyce, Semiconductor device-and-lead structure, U.S. Patent 2,981,877, April 25, 1961 (filed 30 July 1959).
[50] S. Murthy, et al., Large-scale photonic integrated circuit transmitters with monolithically integrated semiconductor optical amplifiers, in: Conf. Proc. OFC2008, OWE1, 2008.
[51] G. Yang, et al., Grating stabilised high power 980 nm pump modules, in: OFC 2007, March 2007 (poster JWA30).
[52] M. Kato, et al., 40-channel transmitter and receiver photonic integrated circuits operating at per channel data rate 12.5 Gbit/s, Electron. Lett. 43 (8) (12 April 2007).
[53] R. Nagarajan, et al., Single chip, 40 channel InP transmitter photonic integrated circuit capable of an aggregate data rate of 1.6 Tb/s, Electron. Lett. 42 (13) (22 June 2006).
[54] P.J. Winzer, R.-J. Essiambre, Advanced optical modulation formats, Proc. IEEE 94 (5) (May 2006) 952.
[55] S. Corzine, et al., 10-channel × 40 Gb/s per channel DQPSK monolithically integrated InP-based transmitter PIC, in: OFC 2008, February 2008 (talk PDP18).
[56] F. Kish, et al., Current status of large-scale InP photonic integrated circuits, IEEE JSTQE, doi:10.1109/JSTQE.2011.2114873.
[57] J.D. McNicol, et al., Single-carrier versus sub-carrier bandwidth considerations for coherent optical systems, in: SPIE Photonics West, January 22–27, 2011, San Francisco, USA, doi:10.1117/12.881631.
[58] R. Nagarajan, et al., 10 channel, 100 G bits/s per channel, dual polarization, coherent QPSK monolithic InP receiver photonic integrated circuit, in: Optical Fiber Conference, March 2011 (to be presented).
[59] J.-C. Antona, S. Bigo, Foreword, in: Special Issue on "Recent Advances on Optical Communications", C. R. Physique 9 (2008) 911–913.
[60] M. Salsi, H. Mardoyan, P. Tran, C. Koebele, E. Dutisseuil, G. Charlet, S. Bigo, 155 × 100 Gbit/s coherent PDM-QPSK transmission over 7200 km, in: Proc. European Conf. on Optical Comm. (ECOC'09), Vienna, 20–24 September 2009 (post-deadline paper PD2.5).
[61] S. Bigo, Multi-terabit/s DWDM terrestrial transmission with bandwidth-limiting optical filtering, in: Special Issue on Optical Communication, IEEE J. Selected Topics Quant. Electron. 10 (2) (March–April 2004) 329–340.
[62] G. Charlet, J. Renaudier, P. Brindel, P. Tran, H. Mardoyan, O. Bertran Pardo, M. Salsi, S. Bigo, Performance comparison of DPSK, P-DPSK, RZ-DQPSK and coherent PDM-QPSK at 40 Gb/s over a terrestrial link, in: Proc. Optical Fiber Communications Conference/National Fiber Optic Engineers Conference (OFC/NFOEC'09), San Diego, 22–26 March 2009 (paper JWA40).
[63] O. Bertran-Pardo, J. Renaudier, G. Charlet, P. Tran, H. Mardoyan, M. Salsi, S. Bigo, Experimental assessment of interactions between nonlinear impairments and polarization mode dispersion in 100-Gb/s coherent systems versus receiver complexity, IEEE Photon. Technol. Lett. 21 (1) (2009) 51–53.
[64] D.N. Godard, Self-recovering equalization and carrier tracking in two-dimensional data communication systems, IEEE Trans. Comm. COM-28 (11) (November 1980) 1867–1875.
[65] A.J. Viterbi, A.M. Viterbi, Nonlinear estimation of PSK-modulated carrier phase with application to burst digital transmission, IEEE Trans. Inform. Theory IT-29 (4) (July 1983) 543–551.
[66] A. Morea, F. Leplingard, T. Zami, N. Brogard, C. Simonneau, B. Lavigne, L. Lorcy, D. Bayart, New transmission systems enabling transparent network perspectives, C. R. Physique 9 (2008) 985–1001.
[67] J.-C. Antona, S. Bigo, Physical design and performance estimation of heterogeneous optical transmission systems, C. R. Physique 9 (2008) 963–984.
[68] M. Joindot, S. Gosselin, Optical transport systems and networks: fundamentals and prospects, C. R. Physique 9 (2008) 914–934.
[69] H.G. Weber, M. Nakazawa (Eds.), Ultrahigh-Speed Optical Transmission Technology, Springer, 2007.
[70] P.J. Winzer, Modulation and multiplexing in optical communication systems, IEEE LEOS Newsletter 23 (1) (2009) 4–10.

[71] A.D. Ellis, Modulation formats which approach the Shannon limit, in: OFC2009 (OMM4).
[72] M. Nakazawa, M. Yoshida, K. Kasai, J. Hongou, 20 Msymbol/s, 64 and 128 QAM coherent optical transmission over 525 km using heterodyne detection with frequency-stabilised laser, Electron. Lett. 43 (2006) 710–712.
[73] M. Nakazawa, T. Yamamoto, K.R. Tamura, 1.28 Tbit/s-70 km OTDM transmission using third- and fourth-order simultaneous dispersion compensation with a phase modulator, Electron. Lett. 36 (24) (2000) 2027–2029.
[74] H.G. Weber, S. Ferber, M. Kroh, C. Schmidt-Langhorst, R. Ludwig, V. Marembert, C. Boerner, F. Futami, S. Watanabe, C. Schubert, Single channel 1.28 Tbit/s and 2.56 Tbit/s DQPSK transmission, Electron. Lett. 42 (3) (2006) 178–179.
[75] M. Nakazawa, T. Hirooka, F. Futami, S. Watanabe, Ideal distortion-free transmission using optical Fourier transformation and Fourier transform-limited optical pulses, IEEE Photon. Technol. Lett. 16 (4) (2004) 1059–1061.
[76] T. Hirano, P. Guan, T. Hirooka, M. Nakazawa, 640 Gbit/s single-polarization DPSK transmission over 525 km with time-domain optical Fourier transformation in a round-trip configuration, in: OFC 2010 (OThD7).
[77] K. Tajima, All-optical switch with switch-off time unrestricted by carrier lifetime, Jpn. J. Appl. Phys. 32 (1993) L1746–L1749.
[78] C. Boerner, V. Marembert, S. Ferber, C. Schubert, C. Schmidt-Langhorst, R. Ludwig, H.G. Weber, 320 Gbit/s clock recovery with electro-optical PLL using a bidirectionally operated electroabsorption modulator as phase comparator, in: OFC 2005 (OTuO3).
[79] C.E. Shannon, A mathematical theory of communication, Bell Syst. Tech. J. 27 (1948) 379–423, and 623-656.
[80] A.H. Gnauck, P.J. Winzer, C.R. Doerr, L.L. Buhl, 10 × 112-Gb/s PDM 16-QAM transmission over 630 km of fiber with 6.2-b/s/Hz spectral efficiency, in: OFC2009 (PDPB8).
[81] H. Takahashi, A. Al Amin, S.L. Jansen, I. Morita, H. Tanaka, DWDM transmission with 7.0-bit/s/Hz spectral efficiency using 8 × 65.1-Gbit/s coherent PDM-OFDM signals, in: OFC 2009 (PDPB7).
[82] M. Nakazawa, S. Okamoto, T. Omiya, K. Kasai, M. Yoshida, 256-QAM (64 Gb/s) coherent optical transmission over 160 km with an optical bandwidth of 5.4 GHz, IEEE Photon. Technol. Lett. 22 (3) (2010) 185–187.
[83] K. Kasai, A. Suzuki, M. Yoshida, M. Nakazawa, Performance improvement of an acetylene (C_2H_2) frequency-stabilised fiber laser, IEICE Electron. Express 3 (2006) 487–492.
[84] H. Nyquist, Certain topics in telegraph transmission theory, AIEE Trans. 47 (1928) 617–644.
[85] J.G. Proakis, Digital Communications, 4th edition, McGraw Hill, 2000.
[86] See e.g. http://www.ciscosecure.net/en/US/solutions/collateral/ns341/ns525/ns537/ns827/White_paper_c11-481360_ns827_Networking_Solutions_White_Paper.html.
[87] P.P. Mitra, J.B. Stark, Nonlinear limits to the information capacity of optical fibre communications, Nature 411 (2001) 1027–1030.
[88] A.D. Ellis, J. Zhao, D. Cotter, Approaching the non-linear Shannon limit, J. Lightwave Technol. 28 (4) (2010) 423–433.
[89] K. Nagayama, et al., Ultra-low-loss (0.1484 dB/km) pure silica core fiber and extension of transmission distance, Electron. Lett. 38 (2002) 1168–1169.
[90] J. Schroeder, R. Mohr, P.B. Macedo, C.J. Montrose, Rayleigh and Brillouin scattering in K2O–SiO2 glasses, J. Am. Ceram. Soc. 56 (1973) 510–514.
[91] K. Tajima, et al., Low Rayleigh scattering P2O5–F–SiO2 glasses, IEEE J. Lightwave Technol. 10 (1992) 1532–1534.
[92] S.R. Nagel, Fiber materials and fabrication methods, in: Stewart E. Miller, Ivan P. Kaminow (Eds.), Optical Fiber Communications II, Academic Press, 1988.
[93] S.F. Carter, et al., Low loss fluoride fiber by reduced pressure casting, Electron. Lett. 26 (2005) 2115–2116.
[94] R.F. Cregan, B.J. Mangan, J.C. Knight, T.A. Birks, P.St.J. Russell, P.J. Roberts, D.C. Allan, Single-mode photonic band gap guidance of light in air, Science 285 (1999) 1537–1539.
[95] P.J. Roberts, F. Couny, H. Sabert, B.J. Mangan, D.P. Williams, L. Farr, M.W. Mason, A. Tomlinson, T.A. Birks, J.C. Knight, P.S.J. Russell, Ultimate low loss of hollow-core photonic crystal fibers, Opt. Express 13 (2005) 236–244.
[96] J.K. Lyngso, et al., Realization of 7-cell hollow core photonic crystal fibers with low-loss in the region between 1.4 μm and 2.3 μm, in: Proc. OECC'09 (paper FS1).
[97] C.J. Hensley, et al., Silica-glass contribution to the effective nonlinearity of hollow-core photonic bandgap fibers, Opt. Express 15 (2007) 3507–3512.
[98] H. Stuart, Dispersive multiplexing in multimode optical fiber, Science 289 (2000) 281–283.
[99] A. Tarighat, R.C.J. Hsu, A. Shah, A.H. Sayed, B. Jalali, Fundamentals and challenges of optical multiple-input multiple-output multimode fiber links, IEEE Communications Magazine 45 (2007) 57–63.
[100] M. Koshiba, K. Saitoh, Y. Kokubun, Heterogeneous multicore fibers: proposal and design principle, IEICE Electronics Express 6 (2009) 98–103.
[101] See postdeadline paper volume, in: Proc. Optical Fiber Communications Conference/National Fiber Optic Engineers Conference (OFC/NFOEC'11), Los Angeles, 6–10 March 2011.
[102] D.P. Hand, P.St.J. Russell, Solitary thermal shock-waves and optical damage in optical fibers: The fiber fuse, Opt. Lett. 13 (1988) 767–769.
[103] N. Hanzawa, K. Kurokawa, K. Tsujikawa, T. Matsui, S. Tomita, Suppression of fiber fuse propagation in photonic crystal fiber (PCF) and hole assisted fiber, in: Technical Digest of Microoptics Conference, 2009, p. M7.
[104] D.C. Hanna, R.M. Percival, I.R. Perry, R.G. Smart, P.J. Suni, J.E. Townsend, A.C. Tropper, Continuous-wave oscillation of a monomode thulium-doped fiber laser, Electron. Lett. 24 (19) (1998) 1222–1223.
[105] M. Digonnet, Rare Earth Doped Fiber Lasers and Amplifiers, Marcel Dekker Inc., 1993.
[106] P.F. Moulton, G.A. Rines, E.V. Slobodtchikov, et al., Tm-doped fiber lasers: Fundamentals and power scaling, IEEE J. Selected Topics Quant. Electron. 15 (2009) 85–92.
[107] M.N. Islam, Raman amplifiers for telecommunications, IEEE J. Selected Topics Quant. Electron. 8 (2002) 548–558.
[108] E.M. Dianov, et al., High-power cw bismuth-fiber lasers, J. Opt. Soc. Amer. B – Opt. Phys. 24 (2007) 1749.
[109] A. Shirakawa, H. Maruyama, K. Ueda, et al., High-power Yb-doped photonic bandgap fiber amplifier at 1150–1200 nm, Optics Express 17 (2009) 447–454.
[110] C. Farrell, C. Codemard, J. Nilsson, A Raman fiber amplifier generating simultaneous gain across multiple Stokes orders by using step shaped optical pulses, in: Europhoton 2008, Paris, France (paper XX).
[111] H. Haus, J.A. Mullen, Phys. Rev. 128 (1962) 2407.
[112] C.M. Caves, Quantum limits in noise in linear amplifiers, Phys. Rev. D 26 (1982) 1817–1839.
[113] K. Croussore, G. Li, Amplitude regeneration of RZ-DPSK signals based on four-wave mixing in fiber, Electron. Lett. 43 (2007) 177–178.
[114] C.J. McKinstrie, M.G. Raymer, S. Radic, M.V. Vasilyev, Quantum mechanics of phase sensitive amplification in a fiber, Opt. Commun. 257 (2006) 146–163.
[115] Z. Tong, C. Lundström, A. Bogris, M. Karlsson, P. Andrekson, D. Syvridis, Measurement of sub-1 dB noise figure in a non-degenerate cascaded phase sensitive fibre parametric amplifier, in: Proceedings of ECOC 2009 (Mo. 1.1.2).
[116] R. Slavik, F. Parmigiani, J. Kakande, C. Lundström, M. Sjödin, P. Andrekson, R. Weerasuriya, S. Sygletos, A.D. Ellis, L. Grüner-Nielsen, D. Jakobsen, S. Herstrøm, R. Phelan, J. O'Gorman, A. Bogris, D. Syvridis, S. Dasgupta, P. Petropoulos, D.J. Richardson, All-optical phase and amplitude regenerator for next-generation telecommunications systems, Nature Photonics 4 (2010) 690–695.